Hybrid Precoder and Combiner Design With Low-Resolution Phase Shifters in mmWave MIMO Systems

Zihuan Wang, *Student Member, IEEE*, Ming Li, *Senior Member, IEEE*, Qian Liu, *Member, IEEE*, and A. Lee Swindlehurst, *Fellow, IEEE*

***Abstract*—Millimeter-wave (mmWave) communications have been considered as a key technology for next-generation cellular systems and Wi-Fi networks because of its advances in providing orders-of-magnitude wider bandwidth than current wireless networks. Economical and energy-efficient analog/digital hybrid precoding and combining transceivers have been often proposed for mmWave massive multiple-input multiple-output (MIMO) systems to overcome the severe propagation loss of mmWave channels. One major shortcoming of existing solutions lies in the assumption of infinite or high-resolution phase shifters (PSs) to realize the analog beamformers. However, low-resolution PSs are typically adopted in practice to reduce the hardware cost and power consumption. Motivated by this fact, in this paper, we investigate the practical design of hybrid precoders and combiners with *low-resolution* PSs in mmWave MIMO systems. In particular, we propose an iterative algorithm which successively designs the low-resolution analog precoder and combiner pair, aiming at conditionally maximizing the spectral efficiency. Then, the digital precoder and combiner are computed based on the obtained effective baseband channel to further enhance the spectral efficiency. In an effort to achieve an even more hardware-efficient large antenna array, we also investigate the design of hybrid beamformers with one-bit resolution (binary) PSs, and present a novel binary analog precoder and combiner optimization algorithm. After analyzing the computational complexity, the proposed low-resolution hybrid beamforming design is further extended to multiuser MIMO communication systems. Simulation results demonstrate the performance advantages of the proposed algorithms compared to existing low-resolution hybrid beamforming designs, particularly for the one-bit resolution PSs scenario.**

***Index Terms*—Millimeter wave (mmWave) communications, hybrid precoder, multiple-input multiple-output (MIMO), phase shifters, one-bit quantization.**

Manuscript received September 13, 2017; revised January 23, 2018 and March 2, 2018; accepted March 3, 2017. Date of publication April 5, 2018; date of current version May 22, 2018. This work was supported in part by the National Natural Science Foundation of China under Grants 61671101, 61601080, and 61761136019 and in part by the Fundamental Research Funds for the Central Universities under Grants DUT15RC(3)121 and DUT17JC10. The work of A. L. Swindlehurst was supported by the National Science Foundation under Grant ECCS-1547155. The guest editor coordinating the review of this paper and approving it for publication was Dr. Christos Masouros. *(Corresponding author: Ming Li.)*

Z. Wang and M. Li are with the School of Information and Communication Engineering, Dalian University of Technology, Dalian 116024, China (e-mail: wangzihuan@mail.dlut.edu.cn; mli@dlut.edu.cn).

Q. Liu is with the School of Computer Science and Technology, Dalian University of Technology, Dalian 116024, China (e-mail: qianliu@dlut.edu.cn).

A. L. Swindlehurst is with the Center for Pervasive Communications and Computing, University of California, Irvine, CA 92697 USA, and also with the Institute for Advanced Study, Technical University of Munich, Munich 80333, Germany (e-mail: swindle@uci.edu).

Color versions of one or more of the figures in this paper are available online at http://ieeexplore.ieee.org.

Digital Object Identifier 10.1109/JSTSP.2018.2819129

I. Introduction

THE past decade has witnessed the exponential growth of data traffic along with the rapid proliferation of wireless devices. This flood of mobile traffic has significantly exacerbated spectrum congestion in current frequency bands, and therefore stimulated intensive interest in exploiting new spectrum bands for wireless communications. Millimeter wave (mmWave) wireless communications, operating in the frequency bands from 30 to 300 GHz, have been demonstrated as a promising candidate to fundamentally solve the spectrum congestion problem [1]–[3].

However, challenges always come along with opportunities. MmWave communications still need to overcome several technical difficulties before real-world deployment. As a negative result of the ten-fold increase of the carrier frequency, the propagation loss in mmWave bands is much higher than that of conventional frequency bands (e.g., 2.4 GHz) due to atmospheric absorption, rain attenuation, and low penetration [4]. From a positive perspective, the smaller wavelength of mmWave signals allows a large antenna array to be packed in a small physical dimension [5]. With the aid of pre/post-coding techniques in massive multiple-input multiple-output (MIMO) systems, the large antenna array can provide sufficient beamforming gain to overcome the severe propagation loss of mmWave channels. It also enables simultaneous transmission of multiple data streams resulting in significant improvements to spectral efficiency.

For MIMO systems operating in conventional cellular frequency bands, the full-digital precoder and combiner are completely realized in the digital domain by adjusting both the magnitude and phase of the baseband signals. However, these conventional full-digital schemes require a large number of expensive and energy-intensive radio frequency (RF) chains, analog-to-digital converters (ADCs), and digital-to-analog converters (DACs). Since mmWave communication systems operate at much higher carrier frequencies and wider bandwidths, the enormous cost and power consumption of the required RF chains and ADCs/DACs make the adoption of full-digital precoding and combining schemes impractical for mmWave systems. Re-

cently, economical and energy-efficient analog/digital hybrid precoders and combiners have been advocated as a promising approach to tackle this issue. The hybrid precoding approaches adopt a large number of phase shifters (PSs) to implement high-dimensional analog precoders to compensate for the severe path-loss at mmWave bands, and a small number of RF chains and DACs to realize low-dimensional digital precoders to provide the necessary flexibility to perform advanced multiplexing/multiuser techniques.

The investigation of hybrid precoder and combiner design has attracted extensive attention in recent years because of its potential energy efficiency for mmWave MIMO communications. The major challenges in designing hybrid precoders are the practical constraints associated with the analog components, such as the requirement that the analog precoding be implemented with constant modulus PSs. Thus, hybrid precoder design typically requires the solution of various matrix factorization problems with constant modulus constraints. In particular, a popular solution to maximize the spectral efficiency of point-to-point transmission is to minimize the Euclidean distance between the hybrid precoder and the full-digital precoder [6]–[13]. Due to the special characteristics of mmWave channels, codebook-based hybrid precoder designs are commonly proposed [14]–[18], in which the columns of the analog precoder are selected from certain candidate vectors, such as array response vectors of the channel and discrete Fourier transform (DFT) beamformers. Extensions of the hybrid beamformer design to multiuser mmWave MIMO systems have also been investigated in [19]–[27].

The aforementioned existing hybrid precoder and combiner designs generally assume that infinite or high-resolution PSs are used for implementing the analog beamformers in order to achieve satisfactory performance close to the full-digital scheme. However, implementing infinite/high-resolution PSs at mmWave frequencies would significantly increase the energy consumption and complexity of the required hardware circuits [28], [29]. Obviously, it is impractical to employ infinite/high-resolution PSs for mmWave systems and real-world analog beamformers will be implemented with low-resolution PSs. Consequently, an important research direction is the exploration of signal processing techniques for hybrid analog/digital architectures that can mitigate the loss of beamforming accuracy due to the low-resolution PSs.

A straightforward approach to obtain the finite-resolution beamformer is to design the infinite-resolution analog beamformer first, and then directly quantize each phase term to a finite set [30]. However, this solution becomes inefficient when the PSs have low resolution. The authors in [31] investigated the hybrid beamforming design with one-bit and two-bit resolution PSs and introduced a novel analog beamformer codebook based on Hadamard transform. However, as we will see in the simulations, there is still a significant performance gap between the method of [31] and the optimal solution. In [32], [33], Sohrabi and Yu proposed to iteratively design the low-resolution hybrid precoder to maximize the spectral efficiency. However, the performance of this algorithm often suffers when one-bit quantized PSs are applied.

In this paper, we first consider the problem of designing hybrid precoders and combiners with low-resolution PSs for a point-to-point mmWave MIMO system. The objective of the proposed algorithm is to minimize the performance loss caused by the low-resolution PSs while maintaining a low computational complexity. To achieve this goal, we propose to successively design the low-resolution analog precoder and combiner pair, aiming at conditionally maximizing the spectral efficiency. Particularly, an iterative phase matching algorithm is introduced to find the optimal low-resolution analog precoder and combiner pair. The major concern and contribution of this work lies in this joint analog precoder and combiner design which has strict low phase resolution and constant magnitude constraints. After finding the optimal analog precoder and combiner, the digital precoder and combiner can be easily computed based on the obtained effective baseband channel to further enhance the spectral efficiency.

Note that the power consumption and cost of the PS are proportional to its resolution. For example, a 4-bit (i.e., 22.5°) resolution PS at mmWave frequencies requires 45-106 mW, while a 3-bit (i.e., 45°) resolution PS needs only 15 mW [29]. In an effort to achieve maximum hardware efficiency, we also investigate the design of hybrid beamformers with one-bit resolution (binary) PSs. Inspired by the findings in [34], we present a binary analog precoder and combiner optimization algorithm under a rank-1 approximation of the interference-included equivalent channel. This algorithm has polynomial complexity in the number of antennas and can achieve almost the same performance as the optimal exhaustive search method. Finally, our investigation of low-resolution hybrid precoders and combiners is extended to multiuser mmWave MIMO systems. Numerical results in the simulation section demonstrate that the proposed algorithms can offer a performance improvement compared with existing low-resolution hybrid beamforming schemes, especially for the one-bit resolution PSs scenario.

Notation: The following notation is used throughout this paper. Boldface lower-case and upper-case letters indicate column vectors and matrices, respectively. $(\cdot)^T$ and $(\cdot)^H$ denote the transpose and transpose-conjugate operations, respectively. $\mathbb{E}\{\cdot\}$ represents statistical expectation. $\mathfrak{Re}\{\cdot\}$ extracts the real part of a complex number; $\mathrm{sign}(\cdot)$ denotes the sign operator; $\mathrm{angle}\{\cdot\}$ represents the phase of a complex number. $\mathbf{I}_L$ indicates an $L \times L$ identity matrix. $\mathbb{C}$ denotes the set of complex numbers. $|\mathbf{A}|$ denotes the determinant of matrix $\mathbf{A}$. $|\mathcal{A}|$ denotes the cardinality of set $\mathcal{A}$. $|a|$ and $\|\mathbf{a}\|$ are the magnitude and norm of a scalar a and vector $\mathbf{a}$, respectively. $\|\mathbf{A}\|_F$ denotes the Frobenius norm of matrix $\mathbf{A}$. Finally, we adopt a Matlab-like matrix indexing notation: $\mathbf{A}(:,i)$ denotes the i-th column of matrix $\mathbf{A}$; $\mathbf{A}(i,j)$ denotes the element of the i-th row and the j-th column of matrix $\mathbf{A}$; $\mathbf{a}(i)$ denotes the i-th element of vector $\mathbf{a}$.

II. System Model and Problem Formulation

A. Point-to-Point mmWave MIMO System Model

We first consider a point-to-point mmWave MIMO system using a hybrid precoder and combiner with low-resolution PSs, as illustrated in Fig. 1. The transmitter employs N_t antennas and N_t^{RF} RF chains to simultaneously transmit N_s data streams to the receiver which is equipped with N_r antennas and N_r^{RF} RF chains. To ensure the spatial multiplexing and the efficiency of

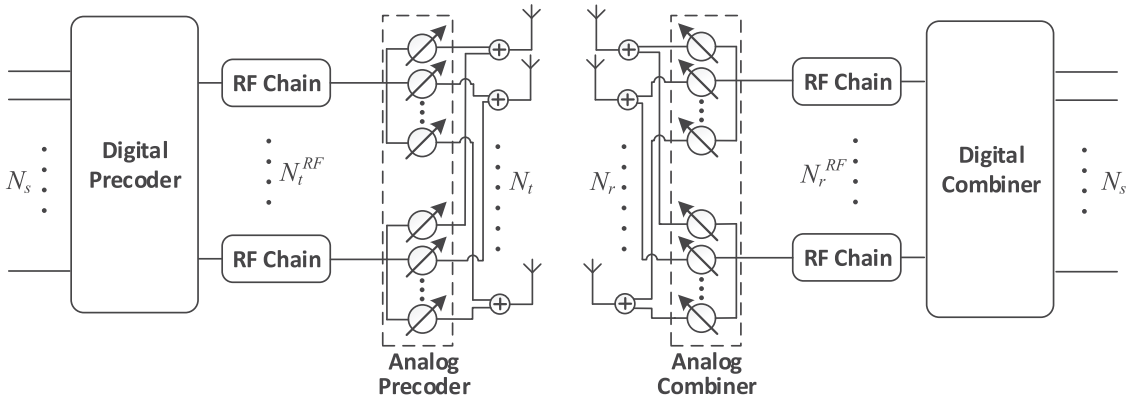

Fig. 1. The point-to-point mmWave MIMO system using hybrid precoder and combiner.

the mmWave MIMO communication with a limited number of RF chains, the number of data streams and the number of RF chains are constrained as $N_s \leq N_t^{RF} = N_r^{RF}$. For conciseness, let N^{RF} denote the number of RF chains at both ends, i.e., $N^{RF} = N_t^{RF} = N_r^{RF}$.

The transmitted symbols are first processed by a baseband digital precoder $\mathbf{F}_{BB} \in \mathbb{C}^{N^{RF} \times N_s}$, then up-converted to the RF domain via N^{RF} RF chains before being precoded with an analog precoder $\mathbf{F}_{RF}$ of dimension $N_t \times N^{RF}$. While the baseband digital precoder $\mathbf{F}_{BB}$ enables both amplitude and phase modifications, the elements of the analog precoder $\mathbf{F}_{RF}$, which are implemented by the PSs, have a constant amplitude $\frac{1}{\sqrt{N_t}}$ and quantized phases: $\mathbf{F}_{RF}(i,j) = \frac{1}{\sqrt{N_t}} e^{j\vartheta_{i,j}}$, in which the phase $\vartheta_{i,j}$ is quantized as $\vartheta_{i,j} \in \mathcal{B} \triangleq \{\frac{2\pi b}{2^B} \mid b = 1, 2, \ldots, 2^B\}$, and B is the number of bits to control the phase. We denote the constraint set of the analog precoder as follows: $\mathbf{F}_{RF}(i,j) \in \mathcal{F} \triangleq \{\frac{1}{\sqrt{N_t}} e^{j\frac{2\pi b}{2^B}} \mid b = 1, 2, \ldots, 2^B\}$. Obviously, a larger number of bits B leads to finer resolution for the PSs and potentially better performance, but also results in higher hardware complexity and power consumption.

The discrete-time transmitted signal can be written in the following form

$$\mathbf{x} = \sqrt{P}\mathbf{F}_{RF}\mathbf{F}_{BB}\mathbf{s}, \tag{1}$$

where $\mathbf{s}$ is the $N_s \times 1$ symbol vector, $\mathbb{E}\{\mathbf{s}\mathbf{s}^H\} = \frac{1}{N_s}\mathbf{I}_{N_s}$, P represents transmit power and this power constraint is enforced by normalizing $\mathbf{F}_{BB}$ such that $\|\mathbf{F}_{RF}\mathbf{F}_{BB}\|_F^2 = N_s$.

We consider a narrow-band slow-fading propagation channel, which yields the following received signal

$$\begin{aligned}\mathbf{y} &= \mathbf{H}\mathbf{x} + \mathbf{n} \\ &= \sqrt{P}\mathbf{H}\mathbf{F}_{RF}\mathbf{F}_{BB}\mathbf{s} + \mathbf{n},\end{aligned} \tag{2}$$

where $\mathbf{y}$ is the $N_r \times 1$ received signal vector, $\mathbf{H}$ is the $N_r \times N_t$ channel matrix, and $\mathbf{n} \sim \mathcal{CN}(\mathbf{0}, \sigma_n^2\mathbf{I}_{N_r})$ is the complex Gaussian noise vector corrupting the received signal.

The receiver employs an analog combiner implemented by the PSs and a digital combiner using N^{RF} RF chains to process the received signal. The signal after the spatial processing has the form

$$\widehat{\mathbf{s}} = \sqrt{P}\mathbf{W}_{BB}^H\mathbf{W}_{RF}^H\mathbf{H}\mathbf{F}_{RF}\mathbf{F}_{BB}\mathbf{s} + \mathbf{W}_{BB}^H\mathbf{W}_{RF}^H\mathbf{n}, \tag{3}$$

where $\mathbf{W}_{RF}$ is the $N_r \times N^{RF}$ analog combiner whose elements have the same constraint as $\mathbf{F}_{RF}$, i.e., $\mathbf{W}_{RF}(i,j) = \frac{1}{\sqrt{N_r}} e^{j\varphi_{i,j}}$, $\varphi_{i,j} \in \mathcal{B}$ and thus $\mathbf{W}_{RF}(i,j) \in \mathcal{W} \triangleq \{\frac{1}{\sqrt{N_r}} e^{j\frac{2\pi b}{2^B}} \mid b = 1, 2, \ldots, 2^B\}$, $\mathbf{W}_{BB}$ is the $N^{RF} \times N_s$ baseband digital combiner.

In this paper, we assume perfect timing and frequency recovery and the channel state information (CSI) of $\mathbf{H}$ is perfectly known to both transmitter and receiver.

B. Problem Formulation

We consider the practical and hardware-efficient scenario in which the PSs have low-resolution to reduce the power consumption and complexity. Under this hardware constraint, we aim to jointly design the hybrid precoder and combiner for a mmWave MIMO system. When Gaussian symbols are transmitted over the mmWave MIMO channel, the achievable spectral efficiency is given by

$$\begin{aligned}R = \log_2\Bigg(\Bigg|\mathbf{I}_{N_s} + \frac{P}{N_s}\mathbf{R}_n^{-1}\mathbf{W}_{BB}^H\mathbf{W}_{RF}^H\mathbf{H}\mathbf{F}_{RF}\mathbf{F}_{BB} \\ \times \mathbf{F}_{BB}^H\mathbf{F}_{RF}^H\mathbf{H}^H\mathbf{W}_{RF}\mathbf{W}_{BB}\Bigg|\Bigg),\end{aligned} \tag{4}$$

where $\mathbf{R}_n \triangleq \sigma_n^2\mathbf{W}_{BB}^H\mathbf{W}_{RF}^H\mathbf{W}_{RF}\mathbf{W}_{BB}$ is the noise covariance matrix after combining. We aim to jointly design the digital beamformers $\mathbf{F}_{BB}$, $\mathbf{W}_{BB}$ as well as the low-resolution analog beamformers $\mathbf{F}_{RF}$, $\mathbf{W}_{RF}$ to maximize the spectral efficiency:

$$\begin{aligned}\left\{\mathbf{F}_{RF}^\star, \mathbf{F}_{BB}^\star, \mathbf{W}_{RF}^\star, \mathbf{W}_{BB}^\star\right\} = \arg\max R \\ \text{s.t.} \quad \mathbf{F}_{RF}(i,j) \in \mathcal{F}, \forall i,j, \\ \mathbf{W}_{RF}(i,j) \in \mathcal{W}, \forall i,j, \\ \|\mathbf{F}_{RF}\mathbf{F}_{BB}\|_F^2 = N_s.\end{aligned} \tag{5}$$

Obviously, the optimization problem (5) is a non-convex NP-hard problem. In the next section, we attempt to decompose the original problem into a series of sub-problems and seek a sub-optimal solution with low-complexity and satisfactory performance.

III. Low-Resolution Hybrid Precoder and Combiner Design

To simplify the joint hybrid precoder and combiner design, the objective problem is decomposed into two separate optimizations. We first focus on the joint design of the analog precoder $\mathbf{F}_{RF}$ and combiner $\mathbf{W}_{RF}$. Then, having the effective baseband channel associated with the obtained optimal analog precoder and combiner, the digital precoder $\mathbf{F}_{BB}$ and combiner $\mathbf{W}_{BB}$ are computed to further maximize the spectral efficiency.

A. Low-Resolution Analog Precoder and Combiner Design

We observe that under the assumption of high signal-to-noise-ratio (SNR), the achievable spectral efficiency in (4) can be approximated as

$$R \approx \log_2\left(\left|\frac{P}{N_s}\mathbf{R}_n^{-1}\mathbf{W}_{BB}^H\mathbf{W}_{RF}^H\mathbf{H}\mathbf{F}_{RF}\mathbf{F}_{BB} \times \mathbf{F}_{BB}^H\mathbf{F}_{RF}^H\mathbf{H}^H\mathbf{W}_{RF}\mathbf{W}_{BB}\right|\right). \quad (6)$$

While the per-antenna SNR in mmWave systems is typically low, the post-combining SNR should be high enough to justify this approximation[1]. In addition, it has been verified in [33] that for large-scale MIMO systems, the optimal analog beamformers are approximately orthogonal, i.e., $\mathbf{F}_{RF}^H\mathbf{F}_{RF} \propto \mathbf{I}_{N^{RF}}$. Besides, it is well known that the optimal full-digital precoder $\mathbf{F}_D$ is obtained from the unitary right singular vectors of the channel matrix $\mathbf{H}$ and $\mathbf{F}_D^H\mathbf{F}_D = \mathbf{I}_{N_s}$. The near-optimal hybrid design should also exhibit the same orthogonality property as $\mathbf{F}_D$, i.e., $\mathbf{F}_{BB}^H\mathbf{F}_{RF}^H\mathbf{F}_{RF}\mathbf{F}_{BB} \approx \mathbf{I}_{N_s}$. This fact allows us to assume that the digital precoder $\mathbf{F}_{BB}$ is also approximately orthogonal, i.e., $\mathbf{F}_{BB}^H\mathbf{F}_{BB} \approx \zeta^2\mathbf{I}_{N_s}$, where ζ^2 is a normalization factor. Similarly, we have $\mathbf{W}_{BB}^H\mathbf{W}_{BB} \approx \xi^2\mathbf{I}_{N_s}$ and $\mathbf{W}_{BB}^H\mathbf{W}_{RF}^H\mathbf{W}_{RF}\mathbf{W}_{BB} \approx \mathbf{I}_{N_s}$. Let $\gamma^2 \triangleq \zeta^2\xi^2$, then (6) can be further simplified as

$$R \approx \log_2\left(\left|\frac{P\gamma^2}{N_s\sigma_n^2}\mathbf{W}_{RF}^H\mathbf{H}\mathbf{F}_{RF}\mathbf{F}_{RF}^H\mathbf{H}^H\mathbf{W}_{RF}\right|\right) \quad (7)$$

$$\overset{(a)}{=} N^{RF}\log_2\left(\frac{P\gamma^2}{N_s\sigma_n^2}\right) + 2\times\log_2\left(\left|\mathbf{W}_{RF}^H\mathbf{H}\mathbf{F}_{RF}\right|\right), \quad (8)$$

where (a) follows since $|\mathbf{X}\mathbf{Y}| = |\mathbf{X}||\mathbf{Y}|$ when $\mathbf{X}$ and $\mathbf{Y}$ are both square matrices. Therefore, the analog precoder and combiner design with low-resolution PSs can be approximately reformulated as:

$$\{\mathbf{F}_{RF}^\star, \mathbf{W}_{RF}^\star\} = \arg\max \log_2\left(\left|\mathbf{W}_{RF}^H\mathbf{H}\mathbf{F}_{RF}\right|\right) \quad \text{s.t.} \quad \mathbf{F}_{RF}(i,j) \in \mathcal{F}, \forall i,j, \quad \mathbf{W}_{RF}(i,j) \in \mathcal{W}, \forall i,j. \quad (9)$$

Unfortunately, the optimization problem (9) is still NP-hard and has exponential complexity $\mathcal{O}(|\mathcal{F}|^{N_t N^{RF}}|\mathcal{W}|^{N_r N^{RF}})$. Therefore, we propose to further decompose this difficult optimization problem into a series of sub-problems, in which each transmit/receive RF chain pair is considered one by one and the analog precoder and combiner for each pair are successively designed.

In particular, we define the singular value decomposition (SVD) of $\mathbf{H}$ as

$$\mathbf{H} = \mathbf{U}\mathbf{\Sigma}\mathbf{V}^H, \quad (10)$$

where $\mathbf{U}$ is an $N_r \times N_r$ unitary matrix, $\mathbf{V}$ is an $N_t \times N_t$ unitary matrix, and $\mathbf{\Sigma}$ is a rectangular diagonal matrix of singular values. Due to the sparse nature of the mmWave channel, the matrix $\mathbf{H}$ is typically low rank. In particular, the effective rank of the channel serves as an upper bound for the number of data streams that the channel can support. With limited number of RF chains, we assume that the channel $\mathbf{H}$ can be well approximated by retaining only the N^{RF} strongest components $\mathbf{H} \approx \widehat{\mathbf{U}}\widehat{\mathbf{\Sigma}}\widehat{\mathbf{V}}^H$, where $\widehat{\mathbf{U}} \triangleq \mathbf{U}(:, 1:N^{RF})$, $\widehat{\mathbf{\Sigma}} \triangleq \mathbf{\Sigma}(1:N^{RF}, 1:N^{RF})$, and $\widehat{\mathbf{V}} \triangleq \mathbf{V}(:, 1:N^{RF})$. Then, the objective in (9) can be converted to

$$\log_2\left(\left|\mathbf{W}_{RF}^H\mathbf{H}\mathbf{F}_{RF}\right|\right) \approx \log_2\left(\left|\mathbf{W}_{RF}^H\widehat{\mathbf{U}}\widehat{\mathbf{\Sigma}}\widehat{\mathbf{V}}^H\mathbf{F}_{RF}\right|\right). \quad (11)$$

[1]In general, the large-scale antenna arrays should be employed in mmWave systems to provide significant beamforming gain to combat the severe propagation losses and ensure sufficient post-combining SNR.

$$\log_2\left(\left|\mathbf{W}_{RF}^H\widehat{\mathbf{U}}\widehat{\mathbf{\Sigma}}\widehat{\mathbf{V}}^H\mathbf{F}_{RF}\right|\right) = \log_2\left(\left|\widehat{\mathbf{\Sigma}}\widehat{\mathbf{V}}^H\mathbf{F}_{RF}\mathbf{W}_{RF}^H\widehat{\mathbf{U}}\right|\right) \quad (12)$$

$$= \log_2\left(\left|\widehat{\mathbf{\Sigma}}\widehat{\mathbf{V}}^H\left[\mathbf{F}_{RF,\setminus l}\,\mathbf{f}_{RF,l}\right]\left[\mathbf{W}_{RF,\setminus l}\,\mathbf{w}_{RF,l}\right]^H\widehat{\mathbf{U}}\right|\right) = \log_2\left(\left|\widehat{\mathbf{\Sigma}}\widehat{\mathbf{V}}^H\mathbf{F}_{RF,\setminus l}\mathbf{W}_{RF,\setminus l}^H\widehat{\mathbf{U}} + \widehat{\mathbf{\Sigma}}\widehat{\mathbf{V}}^H\mathbf{f}_{RF,l}\mathbf{w}_{RF,l}^H\widehat{\mathbf{U}}\right|\right) \quad (13)$$

$$\approx \log_2\left(\left|\left(\widehat{\mathbf{\Sigma}}\widehat{\mathbf{V}}^H\mathbf{F}_{RF,\setminus l}\mathbf{W}_{RF,\setminus l}^H\widehat{\mathbf{U}}\right)\left[\mathbf{I}_{N^{RF}} + \left(\alpha\mathbf{I}_{N^{RF}} + \widehat{\mathbf{\Sigma}}\widehat{\mathbf{V}}^H\mathbf{F}_{RF,\setminus l}\mathbf{W}_{RF,\setminus l}^H\widehat{\mathbf{U}}\right)^{-1}\widehat{\mathbf{\Sigma}}\widehat{\mathbf{V}}^H\mathbf{f}_{RF,l}\mathbf{w}_{RF,l}^H\widehat{\mathbf{U}}\right]\right|\right) \quad (14)$$

$$= \log_2\left(\left|\widehat{\mathbf{\Sigma}}\widehat{\mathbf{V}}^H\mathbf{F}_{RF,\setminus l}\mathbf{W}_{RF,\setminus l}^H\widehat{\mathbf{U}}\right|\right) + \log_2\left(\left|\left[\mathbf{I}_{N^{RF}} + \left(\alpha\mathbf{I}_{N^{RF}} + \widehat{\mathbf{\Sigma}}\widehat{\mathbf{V}}^H\mathbf{F}_{RF,\setminus l}\mathbf{W}_{RF,\setminus l}^H\widehat{\mathbf{U}}\right)^{-1}\widehat{\mathbf{\Sigma}}\widehat{\mathbf{V}}^H\mathbf{f}_{RF,l}\mathbf{w}_{RF,l}^H\widehat{\mathbf{U}}\right]\right|\right) \quad (15)$$

$$= \log_2\left(\left|\mathbf{W}_{RF,\setminus l}^H\widehat{\mathbf{U}}\widehat{\mathbf{\Sigma}}\widehat{\mathbf{V}}^H\mathbf{F}_{RF,\setminus l}\right|\right) + \log_2\left(\left|\left[1 + \mathbf{w}_{RF,l}^H\widehat{\mathbf{U}}\left(\alpha\mathbf{I}_{N^{RF}} + \widehat{\mathbf{\Sigma}}\widehat{\mathbf{V}}^H\mathbf{F}_{RF,\setminus l}\mathbf{W}_{RF,\setminus l}^H\widehat{\mathbf{U}}\right)^{-1}\widehat{\mathbf{\Sigma}}\widehat{\mathbf{V}}^H\mathbf{f}_{RF,l}\right]\right|\right) \quad (16)$$

Next, we write the analog precoding and combining matrices as $\mathbf{F}_{RF} \triangleq [\mathbf{f}_{RF,1} \dots \mathbf{f}_{RF,N^{RF}}]$ and $\mathbf{W}_{RF} \triangleq [\mathbf{w}_{RF,1} \dots \mathbf{w}_{RF,N^{RF}}]$, respectively, where $\mathbf{f}_{RF,l}$ and $\mathbf{w}_{RF,l}, l=1,\dots,N^{RF}$, are the l-th pair of analog precoder and combiner. Furthermore, we denote $\mathbf{F}_{RF,\backslash l}$ as the precoding matrix excluding the l-th precoder vector $\mathbf{f}_{RF,l}$ and $\mathbf{W}_{RF,\backslash l}$ as the combining matrix excluding the l-th combiner vector $\mathbf{w}_{RF,l}$. Then, inspired by [11][2], the formulation (11) can be further transformed to (12)–(16), which are presented at the bottom of the previous page.

In particular, the approximation from (13) to (14) is obtained by taking out the term $\left(\widehat{\mathbf{\Sigma}}\widehat{\mathbf{V}}^H\mathbf{F}_{RF,\backslash l}\mathbf{W}_{RF,\backslash l}^H\widehat{\mathbf{U}}\right)$ as a common factor and adding $\alpha\mathbf{I}_{N^{RF}}$ (α is a very small scalar) to assure the invertibility of $\left(\alpha\mathbf{I}_{N^{RF}} + \widehat{\mathbf{\Sigma}}\widehat{\mathbf{V}}^H\mathbf{F}_{RF,\backslash l}\mathbf{W}_{RF,\backslash l}^H\widehat{\mathbf{U}}\right)$.

Thus, the objective in (9) can be reformulated as:

$$\log_2\left(\left|\mathbf{W}_{RF}^H\mathbf{H}\mathbf{F}_{RF}\right|\right) \approx \log_2\left(\left|\mathbf{W}_{RF,\backslash l}^H\mathbf{H}\mathbf{F}_{RF,\backslash l}\right|\right) + \log_2\left(\left|\mathbf{w}_{RF,l}^H\mathbf{Q}_l\mathbf{f}_{RF,l}\right|\right), \quad (17)$$

where we define the interference-included channel matrix $\mathbf{Q}_l$ as

$$\mathbf{Q}_l \triangleq \widehat{\mathbf{U}}(\alpha\mathbf{I}_{N^{RF}} + \widehat{\mathbf{\Sigma}}\widehat{\mathbf{V}}^H\mathbf{F}_{RF,\backslash l}\mathbf{W}_{RF,\backslash l}^H\widehat{\mathbf{U}})^{-1}\widehat{\mathbf{\Sigma}}\widehat{\mathbf{V}}^H. \quad (18)$$

According to (17), if $\mathbf{F}_{RF,\backslash l}$ and $\mathbf{W}_{RF,\backslash l}$ are known, the problem (9) can be reformulated as finding a corresponding precoder $\mathbf{f}_{RF,l}$ and combiner $\mathbf{w}_{RF,l}$ pair to conditionally maximize the achievable spectral efficiency:

$$\begin{aligned}\left\{\mathbf{f}_{RF,l}^\star, \mathbf{w}_{RF,l}^\star\right\} = \ & \arg\max \ \left|\mathbf{w}_{RF,l}^H\mathbf{Q}_l\mathbf{f}_{RF,l}\right| \\ \text{s.t.} \quad & \mathbf{f}_{RF,l}(i) \in \mathcal{F},\ i=1,\dots,N_t, \\ & \mathbf{w}_{RF,l}(j) \in \mathcal{W},\ j=1,\dots,N_r.\end{aligned} \quad (19)$$

This motivates us to propose an iterative algorithm, which starts with appropriate initial RF precoding and combining matrices then successively designs $\mathbf{f}_{RF,l}$ and $\mathbf{w}_{RF,l}$ according to (19) with an updated $\mathbf{Q}_l$ as in (18) until the algorithm converges.

The complexity of obtaining an optimal solution to (19) for each iteration is now reduced to $\mathcal{O}(|\mathcal{F}|^{N_t}|\mathcal{W}|^{N_r})$, which is still too high. To practically solve the problem (19), in what follows we present an iterative phase matching algorithm, which searches the conditionally optimal phase of each element of the analog precoder $\mathbf{f}_{RF,l}$ and combiner $\mathbf{w}_{RF,l}$. Specifically, we first design the analog precoder $\mathbf{f}_{RF,l}$ assuming the analog combiner $\mathbf{w}_{RF,l}$ is fixed. Let $\vartheta_{l,i}$ be the phase of the i-th element of the analog precoder $\mathbf{f}_{RF,l}$ and let $\varphi_{l,j}$ be the phase of the j-th element of the analog combiner $\mathbf{w}_{RF,l}$. If we temporarily remove the discrete phase constraint, the optimal continuous phase $\tilde{\vartheta}_{l,i}$ of the i-th element of the analog precoder $\mathbf{f}_{RF,l}$ is given by the following proposition, whose proof is provided in Appendix.

Proposition 1: Given the phases $\varphi_{l,j}$, $j=1,\dots,N_r$, of the analog combiner $\mathbf{w}_{RF,l}$ and the phases $\vartheta_{l,u}$, $u=1,\dots,N_t$, $u\neq i$, of the analog precoder $\mathbf{f}_{RF,l}$, the optimal continuous phase $\tilde{\vartheta}_{l,i}$ of the i-th element of analog precoder $\mathbf{f}_{RF,l}$ is

$$\tilde{\vartheta}_{l,i} = \text{angle}\left\{\sum_{j=1}^{N_r} e^{-j\varphi_{l,j}} \sum_{u\neq i}^{N_t} e^{j\vartheta_{l,u}}\mathbf{Q}_l(j,u)\right\} - \text{angle}\left\{\sum_{j=1}^{N_r} e^{-j\varphi_{l,j}}\mathbf{Q}_l(j,i)\right\}. \quad (20)$$

■

Then, after finding the optimal continuous phase $\tilde{\vartheta}_{l,i}$ by (20), we reconsider the discrete phase constraint and find the optimal low-resolution phase $\vartheta_{l,i}$ by quantization:

$$\vartheta_{l,i} = \arg\min_{\hat{\vartheta}_{l,i}\in\mathcal{B}} \left|\tilde{\vartheta}_{l,i} - \hat{\vartheta}_{l,i}\right|. \quad (21)$$

Similarly, if the analog precoder $\mathbf{f}_{RF,l}$ is determined, the optimal continuous phase $\tilde{\varphi}_{l,j}$ of the j-th element of $\mathbf{w}_{RF,l}$ is

$$\tilde{\varphi}_{l,j} = -\text{angle}\left\{\sum_{i=1}^{N_t} e^{j\vartheta_{l,i}} \sum_{u\neq j}^{N_r} e^{-j\varphi_{l,u}}\mathbf{Q}_l(u,i)\right\} = \text{angle}\left\{\sum_{i=1}^{N_t} e^{j\vartheta_{l,i}}\mathbf{Q}_l(j,i)\right\}, \quad (22)$$

and the optimal low-resolution phase $\varphi_{l,j}$ is obtained by

$$\varphi_{l,j} = \arg\min_{\hat{\varphi}_{l,j}\in\mathcal{B}} \left|\tilde{\varphi}_{l,j} - \hat{\varphi}_{l,j}\right|. \quad (23)$$

Motivated by (20)–(23), the iterative procedure to design the precoder $\mathbf{f}_{RF,l}$ and combiner $\mathbf{w}_{RF,l}$ as in (19) is straightforward. With appropriate initial $\vartheta_{l,i}$, $\varphi_{l,j}$, we design the precoder $\mathbf{f}_{RF,l}$ by finding the conditionally optimal phases $\vartheta_{l,i}$ as in (20) and (21). Then, with the obtained $\vartheta_{l,i}$, $i=1,\dots,N_t$, we design the combiner $\mathbf{w}_{RF,l}$ by finding the conditionally optimal phases $\varphi_{l,j}$ as in (22) and (23). We alternate the designs of $\mathbf{f}_{RF,l}$ and $\mathbf{w}_{RF,l}$ iteratively until the obtained phase of each element of $\mathbf{f}_{RF,l}$ and $\mathbf{w}_{RF,l}$ does not change and the convergence is achieved. Note that since in each precoder and combiner design step, the objective function of (19) is monotonically non-decreasing, and thus our proposed algorithm is guaranteed to converge to at least a locally optimal solution. Our extensive simulations indicate that the initialization of the analog beamformers will not notably affect the convergence of the proposed algorithm. Therefore, we suggest initializing the analog beamformers as an all-zero matrix.

The proposed joint low-resolution analog precoder and combiner design is summarized in Algorithm 1.

B. Digital Precoder and Combiner Design

After all analog precoder-combiner pairs have been determined, we can obtain the effective baseband channel $\widetilde{\mathbf{H}}$ as

$$\widetilde{\mathbf{H}} \triangleq \left(\mathbf{W}_{RF}^\star\right)^H\mathbf{H}\mathbf{F}_{RF}^\star, \quad (24)$$

where $\mathbf{F}_{RF}^\star \triangleq [\mathbf{f}_{RF,1}^\star,\dots,\mathbf{f}_{RF,N^{RF}}^\star]$ and $\mathbf{W}_{RF}^\star \triangleq [\mathbf{w}_{RF,1}^\star,\dots,\mathbf{w}_{RF,N^{RF}}^\star]$. For the baseband precoder and combiner design, we define the SVD of the effective baseband channel $\widetilde{\mathbf{H}}$ as

$$\widetilde{\mathbf{H}} = \widetilde{\mathbf{U}}\widetilde{\mathbf{\Sigma}}\widetilde{\mathbf{V}}^H, \quad (25)$$

[2]While [11] focuses on the precoding design and the derivation (7) in [11] involves the precoding matrix only, our objective is joint precoder and combiner design and the development (12)–(16) contains both precoding and combining matrices.

Algorithm 1: Iterative Phase Matching Algorithm for Low-Resolution Analog Precoder and Combiner Design.

Input: $\mathcal{F}$, $\mathcal{W}$, $\mathbf{H}$.
Output: $\mathbf{F}_{RF}^{\star}$ and $\mathbf{W}_{RF}^{\star}$.
1: Initialize $\mathbf{F}_{RF}^{\star}=\mathbf{0}$, $\mathbf{W}_{RF}^{\star}=\mathbf{0}$.
2: **for** $l=1:N^{RF}$ **do**
3: Obtain $\mathbf{F}_{RF,\backslash l}$ from $\mathbf{F}_{RF}^{\star}$ and $\mathbf{W}_{RF,\backslash l}$ from $\mathbf{W}_{RF}^{\star}$.
4: Update $\mathbf{Q}_l=\widehat{\mathbf{U}}(\alpha\mathbf{I}_{N^{RF}}+\widehat{\mathbf{\Sigma}}\widehat{\mathbf{V}}^H\mathbf{F}_{RF,\backslash l}\mathbf{W}_{RF,\backslash l}^H\widehat{\mathbf{U}})^{-1}\widehat{\mathbf{\Sigma}}\widehat{\mathbf{V}}^H$.
5: **while** no convergence of $\vartheta_{l,i}$ and $\varphi_{l,j}$ **do**
6: **for** $i=1:N_t$ **do**
7: Obtain quantized phase $\vartheta_{l,i}$ by (20) and (21).
8: **end for**
9: **for** $j=1:N_r$ **do**
10: Obtain quantized phase $\varphi_{l,j}$ by (22) and (23).
11: **end for**
12: **end while**
13: Construct $\mathbf{f}_{RF,l}^{\star}$ by $\vartheta_{l,i}$ and $\mathbf{w}_{RF,l}^{\star}$ by $\varphi_{l,j}$.
14: **end for**
15: Construct $\mathbf{F}_{RF}^{\star}$ by $\mathbf{f}_{RF,l}^{\star}$ and $\mathbf{W}_{RF}^{\star}$ by $\mathbf{w}_{RF,l}^{\star}$.
16: Goto Step 2 until convergence of $\mathbf{F}_{RF}^{\star}$ and $\mathbf{W}_{RF}^{\star}$ is achieved.

where $\widetilde{\mathbf{U}}$ and $\widetilde{\mathbf{V}}$ are $N^{RF}\times N^{RF}$ unitary matrices, $\widetilde{\mathbf{\Sigma}}$ is an $N^{RF}\times N^{RF}$ diagonal matrix of singular values. Then, to further enhance the spectral efficiency, an SVD-based baseband digital precoder and combiner are employed:

$$\mathbf{F}_{BB}^{\star}=\widetilde{\mathbf{V}}(:,1:N_s), \tag{26}$$

$$\mathbf{W}_{BB}^{\star}=\widetilde{\mathbf{U}}(:,1:N_s). \tag{27}$$

Finally, the baseband precoder is normalized as

$$\mathbf{F}_{BB}^{\star}=\frac{\sqrt{N_s}\mathbf{F}_{BB}^{\star}}{\|\mathbf{F}_{RF}^{\star}\mathbf{F}_{BB}^{\star}\|_F}. \tag{28}$$

IV. One-Bit Resolution Analog Precoder and Combiner Design

In the previous section, we proposed a novel hybrid beamformer design for maximizing the spectral efficiency of a mmWave MIMO system, in which the analog precoder and combiner are implemented with any B-bit resolution PSs. In order to achieve maximum hardware efficiency, in this section we focus on the design of analog precoders and combiners using "one-bit" resolution (binary) PSs, which can maximally reduce the power consumption and simplify the hardware complexity. Although the iterative phase matching algorithm proposed in the previous section can also be applied, a simpler approach is possible in the one-bit case. Therefore, in this section, we present an efficient one-bit resolution analog beamformer design, which can achieve good performance with much lower complexity.

We follow the procedure of the hybrid beamforming design proposed in the previous section, but only modify the optimization problem (19), which attempts to determine the l-th analog precoder and combiner pair. Particularly, we reformulate this analog beamformer design problem (19) with the constraint of one-bit resolution PSs as

$$\left\{\mathbf{f}_{RF,l}^{\star},\mathbf{w}_{RF,l}^{\star}\right\}=\arg\max_{\substack{\mathbf{f}_{RF,l}\in\frac{1}{\sqrt{N_t}}\{\pm1\}^{N_t}\\ \mathbf{w}_{RF,l}\in\frac{1}{\sqrt{N_r}}\{\pm1\}^{N_r}}}\left|\mathbf{w}_{RF,l}^H\mathbf{Q}_l\mathbf{f}_{RF,l}\right|. \tag{29}$$

The optimization problem (29) can be solved through exhaustive search with exponential complexity $\mathcal{O}(2^{N_tN_r})$, which would not be possible with large antenna arrays. Therefore, in the following we attempt to develop an efficient one-bit resolution beamformer design with polynomial complexity in the number of antennas.

We first define the SVD of $\mathbf{Q}_l$ as

$$\mathbf{Q}_l=\sum_{i=1}^{N^{RF}}\lambda_{l,i}\mathbf{p}_{l,i}\mathbf{g}_{l,i}^H, \tag{30}$$

where $\mathbf{p}_{l,i}$ and $\mathbf{g}_{l,i}$ are the i-th left and right singular vectors of $\mathbf{Q}_l$, respectively, and $\lambda_{l,i}$ is the i-th largest singular value, $\lambda_{l,1}\geq\lambda_{l,2}\geq\ldots\geq\lambda_{l,N^{RF}}$. Then, the objective in (29) can be rewritten as

$$|\mathbf{w}_{RF,l}^H\mathbf{Q}_l\mathbf{f}_{RF,l}|=\left|\sum_{i=1}^{N^{RF}}\lambda_{l,i}\mathbf{w}_{RF,l}^H\mathbf{p}_{l,i}\mathbf{g}_{l,i}^H\mathbf{f}_{RF,l}\right|. \tag{31}$$

If we utilize a rank-1 approximation by keeping only the strongest term, i.e., $\mathbf{Q}_l\approx\lambda_{l,1}\mathbf{p}_{l,1}\mathbf{g}_{l,1}^H$, the optimization function in (29) can be approximated by

$$\left\{\mathbf{f}_{RF,l}^{\star},\mathbf{w}_{RF,l}^{\star}\right\}=\arg\max_{\substack{\mathbf{f}_{RF,l}\in\frac{1}{\sqrt{N_t}}\{\pm1\}^{N_t}\\ \mathbf{w}_{RF,l}\in\frac{1}{\sqrt{N_r}}\{\pm1\}^{N_r}}}\left|\mathbf{w}_{RF,l}^H\mathbf{p}_{l,1}\mathbf{g}_{l,1}^H\mathbf{f}_{RF,l}\right|. \tag{32}$$

Since mmWave MIMO channel is sparse in the angular domain and consequently has low-rank property, the interference-included channel matrix $\mathbf{Q}_l$ is also low-rank. Although $\mathbf{Q}_l$ will in general have rank higher than one, we have found that the rank-1 approximation handles the bulk of the cases encountered, and importantly, leads to a much simpler implementation. Therefore, the rank-1 approximation provides an appropriate and useful trade-off between algorithm performance and complexity.

Now, the joint optimization problem (32) can be further decoupled into individually designing the analog precoder $\mathbf{f}_{RF,l}$ and combiner $\mathbf{w}_{RF,l}$:

$$\mathbf{f}_{RF,l}^{\star}=\arg\max_{\mathbf{f}_{RF,l}\in\frac{1}{\sqrt{N_t}}\{\pm1\}^{N_t}}\left|\mathbf{f}_{RF,l}^H\mathbf{g}_{l,1}\right|, \tag{33}$$

$$\mathbf{w}_{RF,l}^{\star}=\arg\max_{\mathbf{w}_{RF,l}\in\frac{1}{\sqrt{N_r}}\{\pm1\}^{N_r}}\left|\mathbf{w}_{RF,l}^H\mathbf{p}_{l,1}\right|. \tag{34}$$

However, solving (33) and (34) by exhaustive search still has exponential complexity in the number of antennas. In order to further reduce the complexity without significant loss of performance, we propose to construct a smaller dimension candidate beamformer set, from which the optimal beamformer can be found with quadradic complexity. In the following, we present this algorithm for the precoder design (33) as an example, while the combiner design (34) follows the same procedure.

We introduce an auxiliary variable $\phi \in [-\pi, \pi)$ and reformulate the optimization problem (33) as:

$$\left\{\phi^\star, \mathbf{f}_{RF,l}^\star\right\} = \arg \max_{\substack{\phi\in[-\pi,\pi) \\ \mathbf{f}_{RF,l}\in\frac{1}{\sqrt{N_t}}\{\pm 1\}^{N_t}}} \Re\mathfrak{e}\left\{\mathbf{f}_{RF,l}^H \mathbf{g}_{l,1} e^{-j\phi}\right\} \quad (35)$$

$$= \arg \max_{\substack{\phi\in[-\pi,\pi) \\ \mathbf{f}_{RF,l}\in\frac{1}{\sqrt{N_t}}\{\pm 1\}^{N_t}}} \sum_{i=1}^{N_t} \mathbf{f}_{RF,l}(i)|\mathbf{g}_{l,1}(i)|\cos(\phi - \psi_i) \quad (36)$$

where ψ_i denotes the phase of $\mathbf{g}_{l,1}(i)$. Obviously, given any $\phi \in [-\pi, \pi)$, the corresponding binary precoder that maximizes (36) is

$$\mathbf{f}_{RF,l}(i) = \frac{1}{\sqrt{N_t}} \text{sign}\left(\cos\left(\phi - \psi_i\right)\right), i = 1, \ldots, N_t. \quad (37)$$

With the conditionally optimal $\mathbf{f}_{RF,l}$ for any given ϕ shown in (37), we will now show that we can always construct a set of N_t candidate binary precoders $\mathcal{F}_l \triangleq \{\mathbf{f}_{l,1}, \ldots, \mathbf{f}_{l,N_t}\}$ and guarantee $\mathbf{f}_{RF,l}^\star \in \mathcal{F}_l$. Then, the maximization in (33) can be carried out over a set of only N_t candidates without loss of performance.

We first define the angles $\widehat{\psi}_i$, $i = 1, \ldots, N_t$, as

$$\widehat{\psi}_i \triangleq \begin{cases} \psi_i - \pi, & \text{if } \psi_i \in \left[\frac{\pi}{2}, \frac{3\pi}{2}\right), \\ \psi_i, & \text{if } \psi_i \in \left[-\frac{\pi}{2}, \frac{\pi}{2}\right), \end{cases} \quad (38)$$

so that $\widehat{\psi}_i \in [-\frac{\pi}{2}, \frac{\pi}{2})$. Then, we map the angles $\widehat{\psi}_i$ to $\widetilde{\psi}_i$, $i = 1, \ldots, N_t$, which are rearranged in ascending order, i.e., $\widetilde{\psi}_1 \leq \widetilde{\psi}_2 \leq \ldots \leq \widetilde{\psi}_{N_t}$. Because of the periodicity of the cosine function, the maximization problem (36) with respect to ϕ can be carried out over any interval of length π. If we construct N_t non-overlapping sub-intervals $[\widetilde{\psi}_1 - \frac{\pi}{2}, \widetilde{\psi}_2 - \frac{\pi}{2}), [\widetilde{\psi}_2 - \frac{\pi}{2}, \widetilde{\psi}_3 - \frac{\pi}{2}), \ldots, [\widetilde{\psi}_{N_t} - \frac{\pi}{2}, \widetilde{\psi}_1 + \frac{\pi}{2})$, then the optimal $\phi^\star$ must be located in one of N_t sub-intervals since the full interval is $[\widetilde{\psi}_1 - \frac{\pi}{2}, \widetilde{\psi}_1 + \frac{\pi}{2})$ of length π. Therefore, the optimization problem (36) can be solved by examining each sub-interval separately.

Assuming the optimal $\phi^\star$ is in the k-th sub-interval, the corresponding optimal binary precoder can be obtained by (37) as $\widetilde{\mathbf{f}}_{l,k}(i) = \frac{1}{\sqrt{N_t}}\text{sign}(\cos(\phi^\star - \widetilde{\psi}_i))$, $i = 1, \ldots, N_t$, and has the form

$$\widetilde{\mathbf{f}}_{l,k} = \frac{1}{\sqrt{N_t}}[\underbrace{1 \ldots 1}_{k} \underbrace{-1 \ldots -1}_{N_t - k}]^T. \quad (39)$$

After that, given the inverse sorting that maps $\widetilde{\psi}_i$ to $\widehat{\psi}_i$, we rearrange the corresponding elements of $\widetilde{\mathbf{f}}_{l,k}$ and obtain $\widehat{\mathbf{f}}_{l,k}$. Then, based on the relationship between ψ_i and $\widehat{\psi}_i$ defined in (38), we can find the conditionally optimal precoder $\mathbf{f}_{l,k}$ by

$$\mathbf{f}_{l,k}(i) \triangleq \begin{cases} -\widehat{\mathbf{f}}_{l,k}(i), & \text{if } \psi_i \in \left[\frac{\pi}{2}, \frac{3\pi}{2}\right), i = 1, \ldots, N_t, \\ \widehat{\mathbf{f}}_{l,k}(i), & \text{if } \psi_i \in \left[-\frac{\pi}{2}, \frac{\pi}{2}\right), i = 1, \ldots, N_t, \end{cases} \quad (40)$$

for the case that $\phi^\star$ is in the k-th sub-interval.

Since the optimal $\phi^\star$ must be located in one of N_t sub-intervals, we can obtain N_t conditionally optimal precoders by examining all N_t sub-intervals and construct a candidate precoder set $\mathcal{F}_l$ as

$$\mathcal{F}_l \triangleq \{\mathbf{f}_{l,1}, \ldots, \mathbf{f}_{l,N_t}\}, \quad (41)$$

which must contain the optimal precoder $\mathbf{f}_{RF,l}^\star$. Therefore, without loss of performance, the problem in (33) can be transformed to an equivalent maximization task over only the set $\mathcal{F}_l$

$$\mathbf{f}_{RF,l}^\star = \arg \max_{\mathbf{f}_{RF,l}\in\mathcal{F}_l} \left|\mathbf{f}_{RF,l}^H \mathbf{g}_{l,1}\right|. \quad (42)$$

Similarly, we can also construct a candidate analog combiner set $\mathcal{W}_l$ and obtain $\mathbf{w}_{RF,l}^\star$ by the same procedure.

The rank-1 solution returned by (42) is based on the rank-1 approximation of the interference-included equivalent channel $\mathbf{Q}_l$. The approximation of $\mathbf{Q}_l$ may cause a performance degradation when we revisit the original problem (29). Therefore, in order to enhance the performance and bridge the gap due to the approximation, we propose to jointly select the precoder and combiner over candidate sets $\mathcal{F}_l$ and $\mathcal{W}_l$ as

$$\left\{\mathbf{f}_{RF,l}^\star, \mathbf{w}_{RF,l}^\star\right\} = \arg \max_{\substack{\mathbf{f}_{RF,l}\in\mathcal{F}_l \\ \mathbf{w}_{RF,l}\in\mathcal{W}_l}} \left|\mathbf{w}_{RF,l}^H \mathbf{Q}_l \mathbf{f}_{RF,l}\right|, \quad (43)$$

which may return the rank-1 or a better solution with polynomial complexity. This low-complexity analog beamformer design with one-bit resolution PSs is summarized in Algorithm 2.

Algorithm 2: One-Bit Resolution Analog Beamformer Design.

Input: $\mathbf{Q}_l$.
Output: $\mathbf{f}_{RF,l}^\star$ and $\mathbf{w}_{RF,l}^\star$.
1: Calculate $\mathbf{p}_{l,1}$ and $\mathbf{g}_{l,1}$ by an SVD of $\mathbf{Q}_l$.
2: Define the angles $\widehat{\psi}_i$, $i = 1, \ldots, N_t$, by (38).
3: Map $\widehat{\psi}_i$ to $\widetilde{\psi}_i$, $i = 1, \ldots, N_t$, in an ascending order.
4: **for** $k = 1 : N_t$ **do**
5: Obtain $\widetilde{\mathbf{f}}_{l,k}$ by (39).
6: Obtain $\widehat{\mathbf{f}}_{l,k}$ from $\widetilde{\mathbf{f}}_{l,k}$ based on inverse mapping from $\widetilde{\psi}_i$ to $\widehat{\psi}_i$, $i = 1, \ldots, N_t$.
7: Obtain $\mathbf{f}_{l,k}$ from $\widehat{\mathbf{f}}_{l,k}$ by (40).
8: **end for**
9: Construct $\mathcal{F}_l = \{\mathbf{f}_{l,1}, \ldots, \mathbf{f}_{l,N_t}\}$.
10: Construct $\mathcal{W}_l$ by a similar procedure as Steps 2-9.
11: Find the optimal $\mathbf{f}_{RF,l}^\star$ and $\mathbf{w}_{RF,l}^\star$ by (43).

V. Complexity Analysis of the Proposed Algorithms

In this section, we analyze the computational complexities of the low-resolution hybrid beamforming designs proposed in the previous sections and compare them with other state-of-the-art algorithms. The computational complexities of our hybrid beamforming approaches can be divided into two parts, i.e., the analog beamformer design and the digital beamformer design. The digital precoder and combiner can be easily obtained by the SVD of the effective channel $\widetilde{\mathbf{H}}$ with computational complexity $\mathcal{O}(N^{RF\,3})$, which is small with a limited number of RF chains and can be neglected. Therefore, we will focus on the complexity analysis of the proposed analog beamformer

TABLE I
COMPLEXITY COMPARISON

	Computational Comlexity
Algorithm 1	$\mathcal{O}\left(N_{iter}^{o}N_{iter}^{i}N^{RF}N^{3}\right)$
Algorithm 2	$\mathcal{O}\left(N_{iter}^{o}N^{RF}N^{3}\right)$
CDM [30]	$\mathcal{O}\left(N_{iter}^{o}N_{iter}^{i}N^{RF^2}N_{s}N^{3}\right)$
HBF [33]	$\mathcal{O}\left(N^{3}+N_{iter}N^{RF^2}N^{2}\right)$

designs. For fair comparison and efficient algorithm analysis, we assume that the number of transmit and receive antennas has the same order of magnitude, i.e., $\mathcal{O}(N_r)=\mathcal{O}(N_t)$, and therefore, let $N=\mathcal{O}(N_r)=\mathcal{O}(N_t)$ denote the number of antennas at both transmitter and receiver sides.

For the analog beamformer design presented in Algorithm 1, the SVD of $\mathbf{H}$ should be executed with computational complexity $\mathcal{O}(N^3)$ before the iterative procedure. Then, in each iteration, the computational complexity includes the calculation of $\mathbf{Q}_l$ which requires $\mathcal{O}(N^{RF}N)$ computations, as well as an inner loop with complexity $\mathcal{O}(N^3)$. Therefore, the overall computational complexity for the low-resolution analog beamformer design in Algorithm 1 is $\mathcal{O}\left(N_{iter}^{o}N_{iter}^{i}N^{RF}N^{3}\right)$, where N_{iter}^{o} and N_{iter}^{i} are the numbers of outer and inner iterations, respectively. In general, N_{iter}^{o} is between 2 and 5 and N_{iter}^{i} is between 3 and 8 to assure convergence.

For the one-bit hybrid beamformer design described in Algorithm 2, the only difference is that each analog beamformer pair is obtained by constructing codebooks rather than the iterative procedure. The complexity of designing a codebook comes from three parts. The first part is from the SVD of $\mathbf{Q}_l$ at Step 1 with complexity $\mathcal{O}(N^3)$. The second part is the sorting operation at Step 3, which has complexity $\mathcal{O}(N^2)$. The last part stems from the analog beamformer selection which requires computational complexity of $\mathcal{O}(N^3)$. Therefore, the computational complexity of Algorithm 2 is $\mathcal{O}\left(N_{iter}^{o}N^{RF}N^{3}\right)$ and N_{iter}^{o} is generally between 2 and 5.

Finally, Table I lists the total computational complexities of the proposed algorithms. For comparison, we also include the complexities of state-of-the-art hybrid design algorithms with quantized PSs: The coordinate descent method (CDM) [30] and the hybrid beamforming approach (HBF) [33]. We can conclude that these algorithms have similar computational complexity.

VI. HYBRID PRECODER AND COMBINER DESIGN FOR MULTIUSER MMWAVE MIMO SYSTEMS

In this section, we consider a mmWave multiuser MIMO uplink system and extend the low-resolution hybrid precoder and combiner designs proposed in the previous sections to the multiuser system.

A. System Model and Problem Formulation

We consider a multiuser mmWave MIMO uplink system as presented in Fig. 2, where a base-station (BS) is equipped with N_r antennas and N^{RF} RF chains and simultaneously serves K mobile users. Due to power consumption and hardware limitations, each mobile user has N_t antennas and a single RF chain to transmit only one data stream to the BS. We further assume the number of RF chains at the BS is equal to the number of users, i.e., $N^{RF}=K$.

Let $\mathbf{f}_{RF,k}$ be the analog precoder of the k-th user, where each element of $\mathbf{f}_{RF,k}$ has a constant magnitude $\frac{1}{\sqrt{N_t}}$ and low-resolution discrete phases, i.e., $\mathbf{f}_{RF,k}(i)\in\mathcal{F}$, $\forall i=1,\ldots,N_t$. The transmitted signal of the k-th user after precoding can be formulated as

$$\mathbf{x}_k=\sqrt{P_k}\mathbf{f}_{RF,k}s_k, \tag{44}$$

where s_k is the symbol of the k-th user, $\mathbb{E}\{|s_k|^2\}=1$, and P_k is the k-th user's transmit power.

Let $\mathbf{H}_k\in\mathbb{C}^{N_r\times N_t}$, $k=1,\ldots,K$, denote the uplink channel from the k-th user to the BS. The received signal at the BS can be written as

$$\mathbf{r}=\sum_{k=1}^{K}\sqrt{P_k}\mathbf{H}_k\mathbf{f}_{RF,k}s_k+\mathbf{n}, \tag{45}$$

where $\mathbf{n}\sim\mathcal{CN}(\mathbf{0},\sigma_n^2\mathbf{I}_{N_r})$ is complex Gaussian noise. The BS first applies an $N_r\times K$ analog combining matrix $\mathbf{W}_{RF}\triangleq[\mathbf{w}_{RF,1}\ldots\mathbf{w}_{RF,K}]$ to process the received signal, in which the analog combiner $\mathbf{w}_{RF,k}$ corresponding to the k-th user is also implemented by low-resolution PSs, i.e., $\mathbf{w}_{RF,k}(j)\in\mathcal{W}$, $j=1,\ldots,N_r$. Then, a baseband digital combiner $\mathbf{w}_{BB,k}\in\mathbb{C}^{K\times 1}$ is employed to retrieve the information of the k-th user. Let $\mathbf{w}_k\triangleq\mathbf{W}_{RF}\mathbf{w}_{BB,k}$ denote the hybrid combiner corresponding to the k-th user. After the combining process at the BS, the estimated symbol of the k-th user can be expressed as

$$\hat{s}_k=\sqrt{P_k}\mathbf{w}_k^H\mathbf{H}_k\mathbf{f}_{RF,k}s_k+\mathbf{w}_k^H\sum_{\substack{i=1\\ i\neq k}}^{K}\sqrt{P_i}\mathbf{H}_i\mathbf{f}_{RF,i}s_i+\mathbf{w}_k^H\mathbf{n}. \tag{46}$$

Given the received signal at the BS in (46), the signal-to-interference-plus-noise ratio (SINR) of the k-th user can be expressed as

$$\gamma_k=\frac{|\sqrt{P_k}\mathbf{w}_k^H\mathbf{H}_k\mathbf{f}_{RF,k}|^2}{\sum_{i=1,i\neq k}^{K}|\sqrt{P_i}\mathbf{w}_k^H\mathbf{H}_i\mathbf{f}_{RF,i}|^2+\sigma_n^2\|\mathbf{w}_k\|^2}, \tag{47}$$

and the achievable sum-rate of the multiuser uplink system is

$$R_u=\sum_{k=1}^{K}\log(1+\gamma_k). \tag{48}$$

We aim to jointly design the analog precoders and combiners implemented by low-resolution PSs as well as the digital combiners to maximize the sum-rate of the uplink multiuser system:

$$\left\{\left\{\mathbf{w}_{RF,k}^{\star},\mathbf{w}_{BB,k}^{\star},\mathbf{f}_{RF,k}^{\star}\right\}_{k=1}^{K}\right\}=\arg\max\sum_{k=1}^{K}\log(1+\gamma_k)$$
$$\text{s.t.}\quad \mathbf{f}_{RF,k}(i)\in\mathcal{F},\ \forall k,i,$$
$$\mathbf{w}_{RF,k}(j)\in\mathcal{W},\ \forall k,j. \tag{49}$$

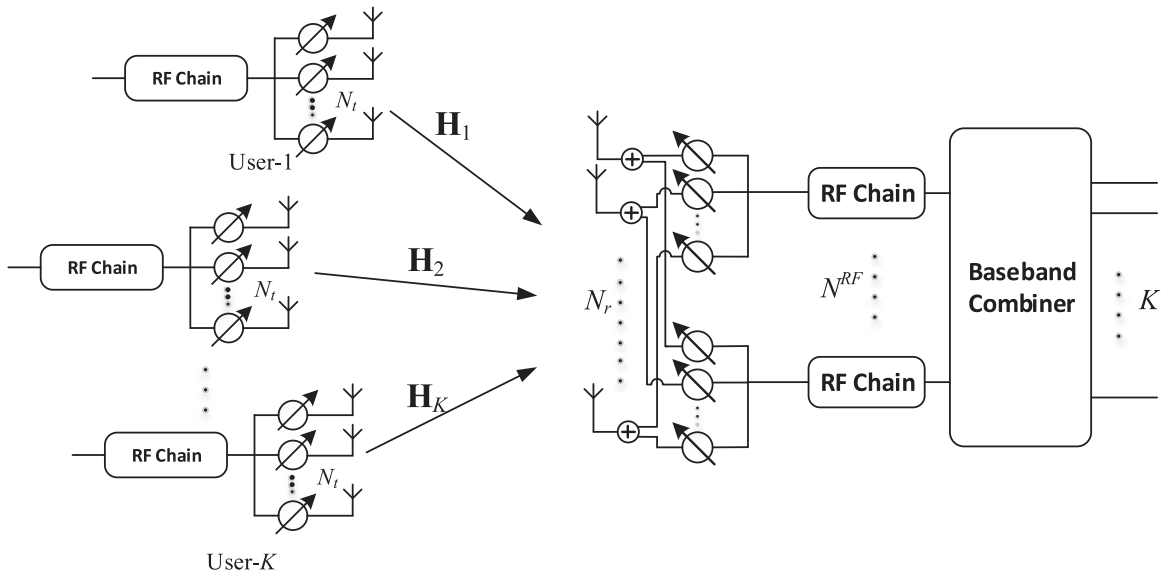

Fig. 2. The multiuser mmWave MIMO system using hybrid precoder and combiner.

B. Low-Resolution Hybrid Precoder and Combiner Design

Obviously, the optimization problem (49) cannot be directly solved. Thus, we adopt an approach similar to [26] and propose to successively design the low-resolution analog beamformer pair for each user, aiming at enhancing the channel gain as well as suppressing the inter-user interference. Then, the baseband combiner at the BS is calculated to further mitigate the interference and maximize the sum-rate.

In particular, for the first user, the analog precoder and combiner pair is designed to maximize the corresponding channel gain, which can be formulated as follows:

$$\begin{aligned}\left\{\mathbf{w}_{RF,1}^{\star},\mathbf{f}_{RF,1}^{\star}\right\} = \arg\max &\left|\mathbf{w}_{RF,1}^{H}\mathbf{H}_1\mathbf{f}_{RF,1}\right| \\ \text{s.t. } &\mathbf{f}_{RF,1}(i)\in\mathcal{F},\, i=1,\ldots,N_t, \\ &\mathbf{w}_{RF,1}(j)\in\mathcal{W},\, j=1,\ldots,N_r. \end{aligned} \tag{50}$$

This analog precoder and combiner design problem can be efficiently solved by the algorithm presented in Section III-A when low-resolution PSs are utilized, or the algorithm proposed in Section IV if only one-bit resolution PSs are available. Then, the analog precoders $\mathbf{f}_{RF,k}$ and combiners $\mathbf{w}_{RF,k}, k=2,3,\ldots,K$, for the remaining $K-1$ users are successively designed by an iterative procedure. In each iteration, we attempt to find the analog beamformer pair that suppresses the interference from the users whose analog beamformers have already been determined. To achieve this goal, the channel of the user whose combiner is to be calculated is projected onto the space orthogonal to the collection of previously designed analog combiners. This approach leads to orthogonal analog combiners that suppress the inter-user interference.

Specifically, to design the k-th user's analog beamformer pair, we first extract the orthonormal components $\mathbf{d}_i$ of the previously determined analog combiners $\mathbf{w}_{RF,i}^{\star}$, $i=1,\ldots,k-1$ by the Gram-Schmidt procedure:

$$\mathbf{q}_i = \mathbf{w}_{RF,i}^{\star} - \sum_{j=1}^{i-1}\mathbf{d}_j^H\mathbf{w}_{RF,i}^{\star}\mathbf{d}_j, \tag{51}$$

$$\mathbf{d}_i = \mathbf{q}_i/\|\mathbf{q}_i\|. \tag{52}$$

Note that $\mathbf{d}_1 = \mathbf{w}_{RF,1}^{\star}$ and $\mathbf{w}_{RF,1}^{\star}$ is the analog combiner calculated for the first user. Then, the combiner components are removed from the k-th user's channel to obtain the modified channel $\widehat{\mathbf{H}}_k$ as

$$\widehat{\mathbf{H}}_k = \left(\mathbf{I}_{N_r} - \sum_{i=1}^{k-1}\mathbf{d}_i\mathbf{d}_i^H\right)\mathbf{H}_k. \tag{53}$$

Finally, based on the modified channel $\widehat{\mathbf{H}}_k$, the analog beamformer pair for the k-th user is found by solving the following optimization using the algorithms proposed in the previous sections:

$$\begin{aligned}\left\{\mathbf{w}_{RF,k}^{\star},\mathbf{f}_{RF,k}^{\star}\right\} = \arg\max &\left|\mathbf{w}_{RF,k}^{H}\widehat{\mathbf{H}}_k\mathbf{f}_{RF,k}\right| \\ \text{s.t. } &\mathbf{f}_{RF,k}(i)\in\mathcal{F},\, i=1,\ldots,N_t, \\ &\mathbf{w}_{RF,k}(j)\in\mathcal{W},\, j=1,\ldots,N_r. \end{aligned} \tag{54}$$

It is also worth pointing out that, instead of just consecutively designing analog beamformers from the first user to the K-th user, an intelligent user ordering might further improve the performance of the proposed procedure. We leave the investigation of this interesting issue for future studies.

After finding the analog beamformers for all users, the effective baseband channel for each user can be obtained as $\mathbf{h}_k^e \triangleq \sqrt{P_k}\left(\mathbf{W}_{RF}^{\star}\right)^H\mathbf{H}_k\mathbf{f}_{RF,k}^{\star}$. Then, a minimum mean square error (MMSE) baseband digital combiner for the k-th user is employed to further suppress the interference:

$$\mathbf{w}_{BB,k}^{\star} = \left[\mathbf{H}^e(\mathbf{H}^e)^H + \sigma^2\left(\mathbf{W}_{RF}^{\star}\right)^H\mathbf{W}_{RF}^{\star}\right]^{-1}\mathbf{h}_k^e, \tag{55}$$

Algorithm 3: Low-Resolution Hybrid Precoder and Combiner Design for Multiuser mmWave Systems.

Input: $\mathcal{F}, \mathcal{W}, \mathbf{H}_k, k = 1, \ldots, K$.

Output: $\mathbf{f}^{\star}_{RF,k}, \mathbf{w}^{\star}_{RF,k}, \mathbf{w}^{\star}_{BB,k}, k = 1, \ldots, K$.

1: Obtain $\mathbf{w}^{\star}_{RF,1}$ and $\mathbf{f}^{\star}_{RF,1}$ for user-1 by solving

$$\left\{\mathbf{w}^{\star}_{RF,1}, \mathbf{f}^{\star}_{RF,1}\right\} = \arg \max_{\substack{\mathbf{w}_{RF,1}(i)\in\mathcal{W} \\ \mathbf{f}_{RF,1}(j)\in\mathcal{F}}} |\mathbf{w}^{H}_{RF,1}\mathbf{H}_1\mathbf{f}_{RF,1}|.$$

2: $\mathbf{d}_1 = \mathbf{w}^{\star}_{RF,1}$.

3: **for** $k = 2 : K$ **do**

4: $\quad \widehat{\mathbf{H}}_k = \left(\mathbf{I}_{N_r} - \sum_{i=1}^{k-1}\mathbf{d}_i\mathbf{d}_i^H\right)\mathbf{H}_k$.

5: $\quad$ Obtain $\mathbf{w}^{\star}_{RF,k}$ and $\mathbf{f}^{\star}_{RF,k}$ for user-k by solving

$$\left\{\mathbf{w}^{\star}_{RF,k}, \mathbf{f}^{\star}_{RF,k}\right\} = \arg \max_{\substack{\mathbf{w}_{RF,k}(i)\in\mathcal{W} \\ \mathbf{f}_{RF,k}(j)\in\mathcal{F}}} |\mathbf{w}^{H}_{RF,k}\widehat{\mathbf{H}}_k\mathbf{f}_{RF,k}|.$$

6: $\quad \mathbf{q}_k = \mathbf{w}^{\star}_{RF,k} - \sum_{i=1}^{k-1}\mathbf{d}_i^H\mathbf{w}^{\star}_{RF,k}\mathbf{d}_i$;

7: $\quad \mathbf{d}_k = \mathbf{q}_k/\|\mathbf{q}_k\|$.

8: **end for**

9: Obtain digital combiners $\mathbf{w}^{\star}_{BB,k}, k = 1, \ldots, K$, by

$$\mathbf{w}^{\star}_{BB,k} = \left[\mathbf{H}^e(\mathbf{H}^e)^H + \sigma^2\left(\mathbf{W}^{\star}_{RF}\right)^H\mathbf{W}^{\star}_{RF}\right]^{-1}\mathbf{h}^e_k.$$

where $\mathbf{H}^e \triangleq [\mathbf{h}^e_1, \ldots, \mathbf{h}^e_K]$. The proposed low-resolution hybrid precoder and combiner design for mmWave multiuser uplink systems is summarized in Algorithm 3.

For a multiuser downlink system, a similar approach can be applied by slightly modifying the formulation of the proposed algorithm thanks to the duality of the uplink and downlink channels. For conciseness, we will not provide an algorithm for the downlink case here, but we present some simulation results for this case in the next section.

VII. Simulation Results

In this section, we provide simulation results for the proposed joint hybrid precoder and combiner designs with low-resolution PSs for point-to-point mmWave systems as well as multiuser mmWave systems. MmWave channels are expected to be sparse and have a limited number of propagation paths. In the simulations, we adopt a geometric channel model with L paths [33]. In particular, the discrete-time narrow-band mmWave channel $\mathbf{H}$ is formulated as

$$\mathbf{H} = \sqrt{\frac{N_t N_r}{L}}\sum_{i=1}^{L}\alpha_i\mathbf{a}_r(\theta_i^r)\mathbf{a}_t(\theta_i^t)^H, \tag{56}$$

where $\alpha_i \sim \mathcal{CN}(0, \frac{1}{L})$ are the independent and identically distributed complex gains of the i-th propagation path (ray). θ_i^t and $\theta_i^r \in [-\frac{\pi}{2}, \frac{\pi}{2}]$ are the angles of departure (AoDs) and the angles of arrival (AoAs), respectively. Finally, the array response vectors $\mathbf{a}_t(\theta^t)$ and $\mathbf{a}_r(\theta^r)$ depend on the antenna array geometry. We assume that the commonly used uniform linear arrays (ULAs) are employed, and the transmit antenna array response vector $\mathbf{a}_t(\theta^t)$ and the receive antenna array response vector

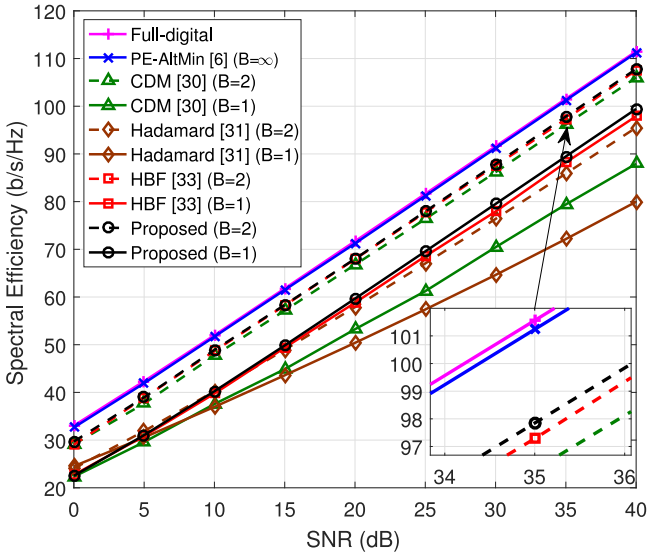

Fig. 3. Spectral efficiency versus SNR ($N_t = 64$, $N_r = 64$, $N^{RF} = 6$, $N_s = 6$).

$\mathbf{a}_r(\theta^r)$ can be written as

$$\mathbf{a}_t(\theta^t) = \frac{1}{\sqrt{N_t}}[1, e^{j\frac{2\pi}{\lambda}d\sin(\theta^t)}, \ldots, e^{j(N_t-1)\frac{2\pi}{\lambda}d\sin(\theta^t)}]^T, \tag{57}$$

$$\mathbf{a}_r(\theta^r) = \frac{1}{\sqrt{N_r}}[1, e^{j\frac{2\pi}{\lambda}d\sin(\theta^r)}, \ldots, e^{j(N_r-1)\frac{2\pi}{\lambda}d\sin(\theta^r)}]^T, \tag{58}$$

respectively, where λ is the signal wavelength, and d is the distance between antenna elements. In the following simulations, we consider an environment with $L = 6$ scatterers between the transmitter and the receiver. The antenna spacing is $d = \frac{\lambda}{2}$.

A. Simulation Results of a Point-to-Point mmWave System

We first consider a point-to-point mmWave communication system, in which the transmitter and receiver are both equipped with 64-antenna ULAs. The numbers of RF chains at the transmitter and receiver are $N^{RF} = 6$ and the number of data streams is also assumed to be $N_s = 6$ to ensure the efficiency of the spatial multiplexing.

Fig. 3 shows the average spectral efficiency versus SNR over 10^6 channel realizations. We evaluate the spectral efficiency of the algorithm proposed in Section III for the case of 2-bit ($B = 2$) resolution PSs[3] and the algorithm proposed in Section IV for the case of 1-bit ($B = 1$) resolution PSs. For comparison purposes, we also plot the spectral efficiency of three state-of-the-art low-resolution hybrid beamformer designs: The coordinate descent method (CDM) algorithm in [30], the Hadamard codebooks design (Hadamard) in [31], and the hybrid beamforming (HBF) algorithm in [33]. To the best of our knowledge, the algorithm in [33] achieves the best performance

[3]While the proposed algorithm in Section III is for any B-bit resolution PSs, we only focus on the low-resolution case ($B = 2$) in the simulation studies.

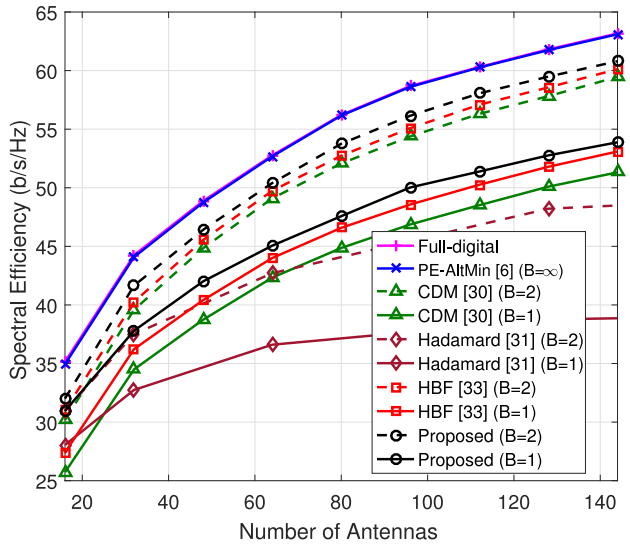

Fig. 4. Spectral efficiency versus number of antennas ($N^{RF} = 4$, $N_s = 4$, SNR $= 20$ dB).

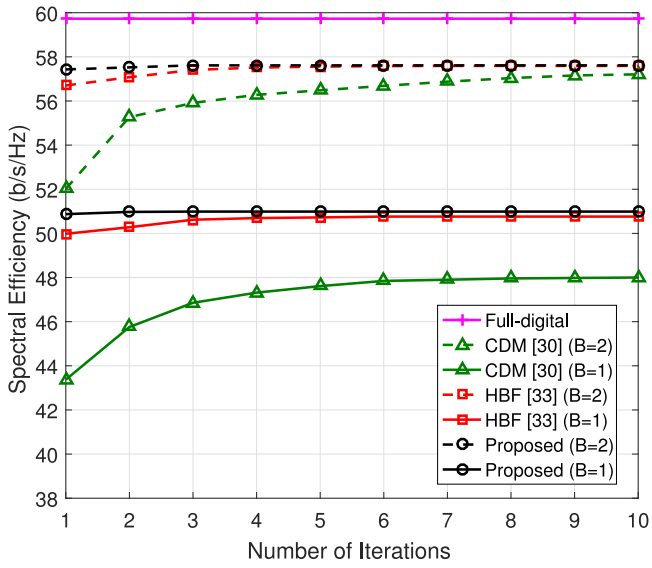

Fig. 5. Spectral efficiency versus number of iterations ($N_t = 64$, $N_r = 64$, $N^{RF} = 4$, $N_s = 4$, SNR $= 20$ dB).

with low-resolution PSs in the existing literature. The performance of a full-digital approach using SVD-based beamforming and the hybrid beamforming scheme with infinite-resolution ($B = \infty$) PSs using the phase extraction (PE-AltMin) algorithm in [6] are also included as performance benchmarks. Fig. 3 illustrates that the proposed algorithm outperforms the competitors, particularly for the case of 1-bit resolution PSs. Moreover, it can be observed that the proposed algorithm with $B = 2$ achieves performance close to optimal full-digital beamforming and hybrid beamforming with infinite-resolution PSs. For additional simulation validation, Fig. 4 illustrates the spectral efficiency versus the number of antennas and similar conclusions can be drawn.

In order to illustrate the convergence of the proposed algorithm, we show the spectral efficiency versus the number of iterations in Fig. 5, which also includes other algorithms for comparison. It is observed that our proposed algorithms can achieve satisfactory performance even after only one iteration and converge quickly within three iterations. The convergence speed of our proposed algorithms is much faster than the other two iterative schemes, which is a highly favorable property. In Fig. 6, we show the spectral efficiency as a function of B to illustrate the impact of the resolution of PSs on the spectral efficiency. We also include the directly quantized version of PE-AltMin (PE-AltMin-DQ) for the comparison purpose. As expected, increasing the resolution of PSs will improve the system performance, but using only $B = 3$ bits is sufficient to closely approach the performance of the ideal unquantized case. Beyond $B = 3$, the additional cost and complexity associated with using higher-resolution PSs is not warranted given the very marginal increase in spectral efficiency. Moreover, our proposed algorithms outperform the other low-resolution beamforming methods for all PS resolutions.

To examine the impact of the approximations used in deriving the proposed one-bit resolution hybrid beamformer scheme, in Fig. 7 we compare it with the optimal exhaustive search

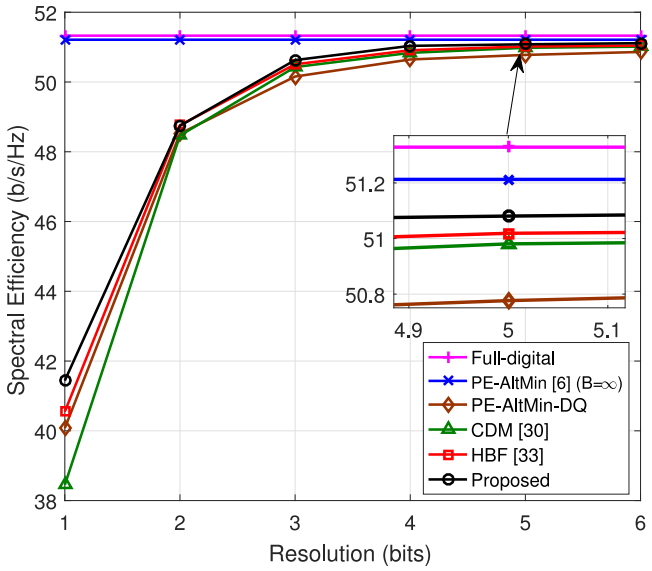

Fig. 6. Spectral efficiency versus resolution of PSs ($N_t = 64$, $N_r = 64$, $N^{RF} = 4$, $N_s = 4$, SNR $= 20$ dB).

approach. The number of antennas at both transmitter and receiver is chosen to be 8 and the number of data streams is $N_s = 1$. A relatively simple case is examined here due to the exponential complexity of the exhaustive search method. We see from Fig. 7 that the spectral efficiency achieved by the proposed algorithm is the same as that of the optimal exhaustive search method, suggesting that the proposed hybrid beamforming algorithm with one-bit resolution PSs can provide optimal or near-optimal performance. Finally, Fig. 8 illustrates the spectral efficiency of the proposed algorithms versus the number of data streams N_s with a fixed number of RF chains $N^{RF} = 8$ ($N_s \leq N^{RF}$). These simulation results verify that the proposed algorithms can achieve satisfactory performance for the cases of $N_s \leq N^{RF}$.

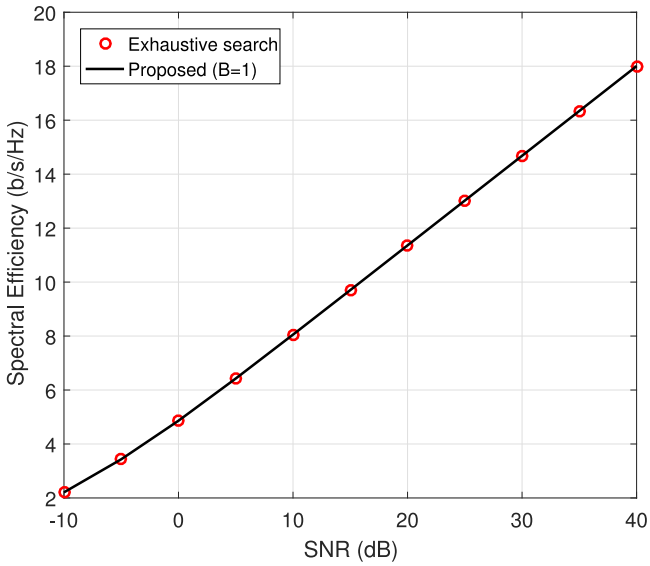

Fig. 7. Spectral efficiency versus SNR ($N_t = 8$, $N_r = 8$, $N^{RF} = 1$, $N_s = 1$, $B = 1$).

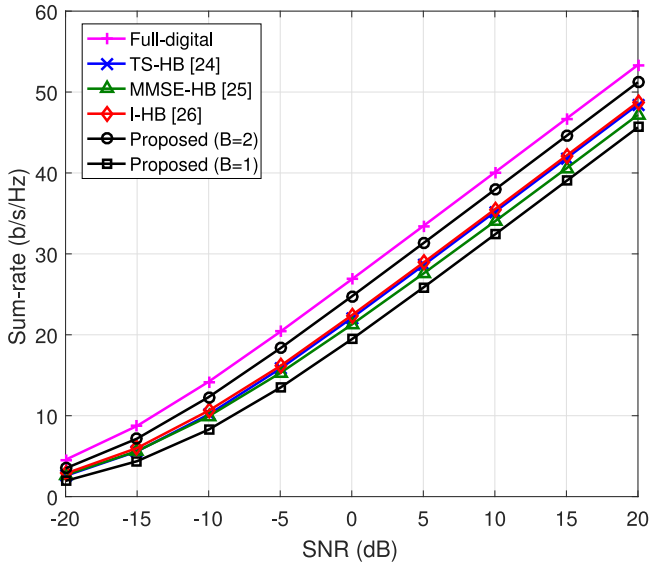

Fig. 9. Spectral efficiency versus SNR for the uplink systems ($N_r = 64$, $N_t = 16$, $N^{RF} = 4$, $K = 4$).

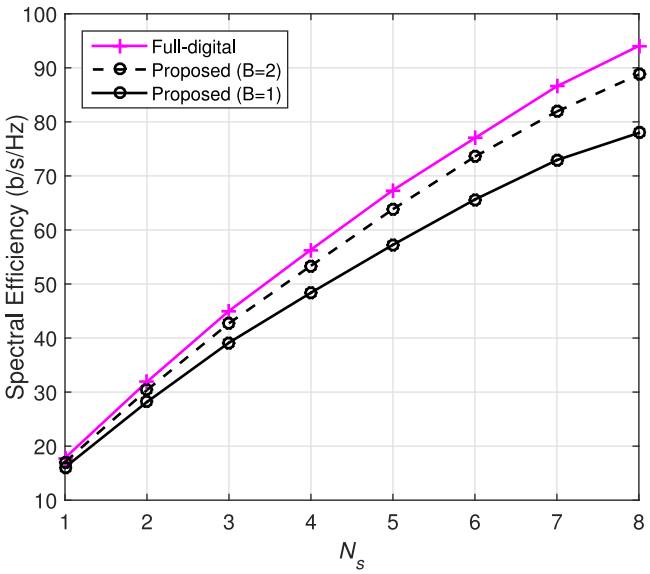

Fig. 8. Spectral efficiency versus N_s ($N_t = 64$, $N_r = 64$, $N^{RF} = 8$, SNR $= 20$ dB).

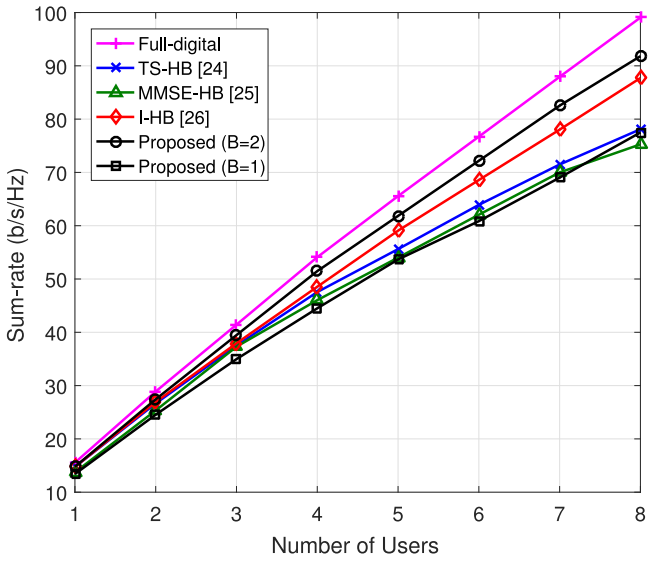

Fig. 10. Spectral efficiency versus K for the uplink systems ($N_r = 64$, $N_t = 16$, $N^{RF} = K$, SNR $= 20$ dB).

B. Simulation Results of a Multiuser mmWave System

Next, we evaluate the performance of the proposed low-resolution hybrid beamformer design algorithm in a multiuser uplink system. We assume that there are $K = 4$ users, each of which is equipped with $N_t = 16$ antennas and only one RF chain to transmit a single data stream. The BS has $N_r = 64$ antennas and $N^{RF} = 4$ RF chains. Fig. 9 illustrates the sum-rate versus SNR for various hybrid beamformer designs. In particular, we include three state-of-the-art multiuser hybrid beamforming approaches for comparison: *i*) Two-stage hybrid beamforming (TS-HB) in [24], *ii*) MMSE-based hybrid beamforming (MMSE-HB) in [25], and *iii*) iterative hybrid beamforming (I-HB) in [26]. All three algorithms are codebook-based approaches and the size of the beamsteering codebook is set at 32 (i.e., $B = 5$ quantization bits). It can be observed from Fig. 9 that our proposed low-resolution hybrid beamforming design outperforms the other three algorithms using only 2-bit resolution PSs. Moreover, the performance with 1-bit resolution PSs is also comparable. Fig. 10 further shows the sum-rate versus the number of users K. From Fig. 10, we see that our proposed algorithm with 2-bit resolution PSs always outperforms the other codebook-based algorithms. Furthermore, even with 1-bit resolution PSs, the proposed algorithm can still achieve competitive performance compared with the TS-HB and MMSE-HB approaches when $K > 5$. The algorithms developed in this paper can also be extended in a straightforward way to multiuser

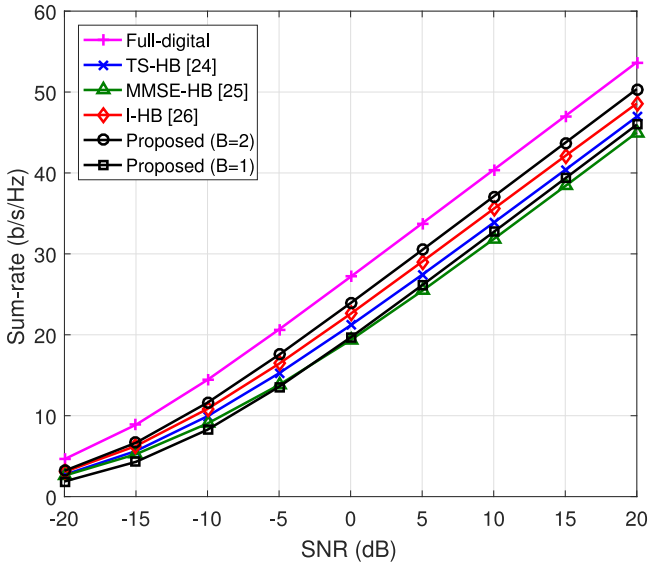

Fig. 11. Spectral efficiency versus SNR for the downlink systems ($N_t = 64$, $N_r = 16$, $N^{RF} = 4$, $K = 4$).

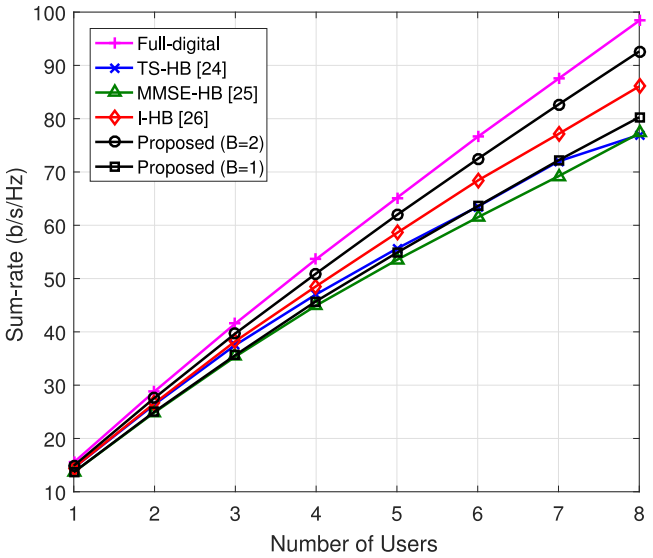

Fig. 12. Spectral efficiency versus K for the downlink systems ($N_t = 64$, $N_r = 16$, $N^{RF} = K$, SNR = 20 dB).

downlink systems. Figs. 11 and 12 show the performance of our approach in the downlink, and conclusions similar to the uplink can be drawn in this case as well.

VIII. Conclusion

This paper considered the problem of hybrid precoder and combiner design for mmWave MIMO systems with low-resolution quantized PSs. We proposed an efficient iterative algorithm which successively designs the low-resolution analog precoder and combiner pair for each data stream. Then, the digital precoder and combiner were computed based on the obtained effective baseband channel to further enhance the spectral efficiency. The design of low-resolution hybrid beamformers for multiuser MIMO communication systems was also investigated. Simulation results verified the effectiveness of the proposed algorithms, particularly for scenarios in which one-bit resolution PSs are used.

Appendix
Proof of Proposition 1

The optimization problem (19) can be equivalently formulated as

$$\max \left| \frac{1}{\sqrt{N_t N_r}} \sum_{j=1}^{N_r} e^{-j\varphi_{l,j}} \sum_{i=1}^{N_t} e^{j\vartheta_{l,i}} \mathbf{Q}_l(j,i) \right|. \tag{59}$$

By discarding the constant coefficient $1/\sqrt{N_t N_r}$, (59) can be further transformed as

$$\max \left| \sum_{j=1}^{N_r} e^{-j\varphi_{l,j}} \left\{ e^{j\vartheta_{l,i}} \mathbf{Q}_l(j,i) + \sum_{u \neq i}^{N_t} e^{j\vartheta_{l,u}} \mathbf{Q}_l(j,u) \right\} \right|. \tag{60}$$

Since the term $e^{j\vartheta_{l,i}}$ does not involve the summation index j, it can be put outside the first summation, resulting in

$$\max \left| e^{j\vartheta_{l,i}} \sum_{j=1}^{N_r} e^{-j\varphi_{l,j}} \mathbf{Q}_l(j,i) + \sum_{j=1}^{N_r} e^{-j\varphi_{l,j}} \sum_{u \neq i}^{N_t} e^{j\vartheta_{l,u}} \mathbf{Q}_l(j,u) \right|. \tag{61}$$

Obviously, the optimal value of $\vartheta_{l,i}$ makes the phases of the first and second term equal to obtain the largest amplitude, and (20) is proved. ■

References

[1] Z. Pi and F. Khan, "An introduction to millimeter-wave mobile broadband systems," *IEEE Commun. Mag.*, vol. 49, no. 6, pp. 101–107, Jun. 2011.
[2] T. Rappaport *et al.*, "Millimeter wave mobile communications for 5G cellular: It will work!" *IEEE Access*, vol. 1, pp. 335–349, 2013.
[3] A. Lee Swindlehurst, E. Ayanoglu, P. Heydari, and F. Capolino, "Millimeter-wave massive MIMO: The next wireless revolution?" *IEEE Commun. Mag.*, vol. 52, no. 9, pp. 56–62, Sep. 2014.
[4] T. S. Rappapport, G. R. MacCartney, M. K. Samimi, and S. Sun, "Wideband millimeter-wave propagation measurements and channel models for future wireless communication system design," *IEEE Trans. Commun.*, vol. 63, no. 9, pp. 3029–3056, Sep. 2015.
[5] R. W. Heath, N. González-Prelcic, S. Rangan, W. Roh, and A. M. Sayeed, "An overview of signal processing techniques for millimeter wave MIMO systems," *IEEE J. Sel. Topics Signal Process.*, vol. 10, no. 3, pp. 436–453, Apr. 2016.
[6] X. Yu, J.-C. Shen, J. Zhang, and K. B. Letaief, "Alternating minimization algorithms for hybrid precoding in millimeter wave MIMO systems," *IEEE J. Sel. Topics Signal Process.*, vol. 10, no. 3, pp. 485–500, Apr. 2016.
[7] C. Rusu, R. Méndez-Rial, N. González-Prelcic, and R. W. Heath, Jr., "Low complexity hybrid precoding strategies for millimeter wave communication systems," *IEEE Trans. Wireless Commun.*, vol. 15, no. 12, pp. 8380–8393, Sep. 2016.
[8] R. López-Valcarce, N. González-Prelcic, C. Rusu, and R. W. Heath, "Hybrid precoders and combiners for mmWave MIMO systems with per-antenna power constraints." in *Proc. IEEE Global Commun. Conf.*, Washington, DC, USA, Dec. 2016, pp. 1–6.
[9] C.-E. Chen, "An iterative hybrid transceiver design algorithm for millimeter wave MIMO systems," *IEEE Wireless Commun. Lett.*, vol. 4, no. 3, pp. 285–288, Jun. 2015.
[10] W. Ni, X. Dong, and W.-S. Lu, "Near-optimal hybrid processing for massive MIMO systems via matrix decomposition," *IEEE Trans. Signal Process.*, vol. 65, no. 15, pp. 3922–3933, Aug. 2017.

[11] X. Gao, L. Dai, S. Han, C.-L. I, and R. W. Heath, Jr., "Energy-efficient hybrid analog and digital precoding for mmWave MIMO systems with large antenna arrays," *IEEE J. Sel. Areas Commun.*, vol. 34, no. 4, pp. 998–1009, Apr. 2016.
[12] L. Dai, X. Gao, J. Quan, S. Han, and C.-L. I, "Near-optimal hybrid analog and digital precoding for downlink mmWave massive MIMO systems," in *Proc. IEEE Int. Conf. Commun.*, London, U.K., Jun. 2015, pp. 1334–1339.
[13] S. He, C. Qi, Y. Wu, and Y. Huang, "Energy-efficient transceiver design for hybrid sub-array architecture MIMO systems," *IEEE Access*, vol. 4, pp. 9895–9905, 2016.
[14] O. E. Ayach, S. Rajagopal, S. Abu-Surra, Z. Pi, and R. W. Heath, Jr., "Spatially sparse precoding in millimeter wave MIMO systems," *IEEE Trans. Wireless Commun.*, vol. 13, no. 3, pp. 1499–1513, Mar. 2014.
[15] A. Alkhateeb, O. El Ayach, G. Leus, and R. W. Heath, Jr., "Channel estimation and hybrid precoding for millimeter wave cellular systems," *IEEE J. Sel. Topics Signal Process.*, vol. 8, no. 5, pp. 831–846, Oct. 2014.
[16] C. Rusu, R. Méndez-Rial, N. González-Prelcic, and R. W. Heath, Jr., "Low complexity hybrid sparse precoding and combining in millimeter wave MIMO systems," in *Proc. IEEE Int. Conf. Commun.*, London, U.K., Jun. 2015, pp. 1340–1345.
[17] J.-C. Chen, "Efficient codebook-based beamforming algorithm for millimeter-wave massive MIMO systems," *IEEE Trans. Veh. Technol.*, vol. 66, no. 9, pp. 7809–7817, Sep. 2017.
[18] X. Gao, L. Dai, C. Yuen, and Z. Wang, "Turbo-like beamforming based on Tabu search algorithm for millimeter-wave massive MIMO systems," *IEEE Trans. Veh. Technol.*, vol. 65, no. 7, pp. 5731–5737, Jul. 2016.
[19] S. Han, C.-L. I, Z. Xu, and C. Rowell, "Large-scale antenna systems with hybrid analog and digital beamforming for millimeter wave 5G," *IEEE Commun. Mag.*, vol. 53, no. 1, pp. 186–194, Jan. 2015.
[20] A. Li and C. Masouros, "Hybrid analog-digital millimeter-wave MU-MIMO transmission with virtual path selection," *IEEE Commun. Lett.*, vol. 21, no. 2, pp. 438–441, Feb. 2017.
[21] L. Liang, W. Xu, and X. Dong, "Low-complexity hybrid precoding in massive multiuser MIMO systems," *IEEE Wireless Commun. Lett.*, vol. 3, no. 6, pp. 653–656, Dec. 2014.
[22] A. Li and C. Masouros, "Hybrid precoding and combining design for millimeter-wave multi-user MIMO based on SVD," in *Proc. IEEE Int. Conf. Commun.*, Paris, France, May 2017, pp. 1–6.
[23] M. Kim and Y. H. Lee, "MSE-based hybrid RF/baseband processing for millimeter-wave communication systems in MIMO interference channels," *IEEE Trans. Veh. Technol.*, vol. 64, no. 6, pp. 2714–2720, Jun. 2015.
[24] A. Alkhateeb, G. Leus, and R. W. Heath Jr., "Limited feedback hybrid precoding for multi-user millimeter wave systems," *IEEE Trans. Wireless Commun.*, vol. 14, no. 11, pp. 6481–6494, Nov. 2015.
[25] D. H. N. Nguyen, L. B. Le, and T. Le-Ngoc, "Hybrid MMSE precoding for mmWave multiuser MIMO systems," in *Proc. IEEE Int. Conf. Commun.*, Kuala Lumpur, Malaysia, May 2016, pp. 1–6.
[26] Z. Wang, M. Li, X. Tian, and Q. Liu, "Iterative hybrid precoder and combiner design for mmWave multiuser MIMO systems," *IEEE Commun. Lett.*, vol. 21, no. 7, pp. 1581–1584, Jul. 2017.
[27] T. E. Bogale, L. B. Le, A. Haghighat, and L. Vandendorpe, "On the number of RF chains and phase shifters, and scheduling design with hybrid analog-digital beamforming," *IEEE Trans. Wireless Commun.*, vol. 15, no. 5, pp. 3311–3326, May 2016.
[28] A. S. Y. Poon and M. Taghivand, "Supporting and enabling circuits for antenna arrays in wireless communications," *Proc. IEEE*, vol. 100, no. 7, pp. 2207–2218, Jul. 2012.
[29] R. Méndez-Rial, C. Rusu, N. González-Prelcic, and A. Alkhateeb, "Hybrid MIMO architectures for millimeter wave communications: Phase shifters or switches?" *IEEE Access*, vol. 4, pp. 247–267, 2016.
[30] J.-C. Chen, "Hyrbrid beamforming with discrete phase shifters for millimeter-wave massive MIMO systems," *IEEE Trans. Veh. Technol.*, vol. 66, no. 8, pp. 7604–7608, Aug. 2017.
[31] H. Seleem, A. I. Sulyman, and A. Alsanie, "Hybrid precoding-beamforming design with hadamard RF codebook for mmWave large-scale MIMO systems," *IEEE Access*, vol. 5, pp. 6813–6823, 2017.
[32] F. Sohrabi and W. Yu, "Hybrid beamforming with finite-resolution phase shifters for large-scale MIMO systems," in *Proc. IEEE Workshop Signal Process. Adv. Wireless Commun.*, Stockholm, Sweden, Jun. 2015, pp. 136–140.
[33] F. Sohrabi and W. Yu, "Hybrid digital and analog beamforming design for large-scale antenna arrays," *IEEE J. Sel. Topics Signal Process.*, vol. 10, no. 3, pp. 501–513, Apr. 2016.
[34] G. N. Karystinos and D. A. Pados, "Rank-2-optimal adaptive design of binary spreading codes," *IEEE Trans. Inf. Theory*, vol. 53, no. 9, pp. 3075–3080, Sep. 2007.

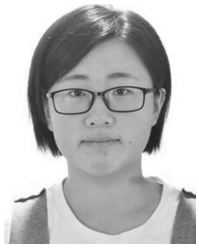

Zihuan Wang (S'17) received the B.S. degree in electronics information engineering from the Dalian University of Technology, Dalian, China, in 2017. She is currently working toward the M.S. degree with the School of Information and Communication Engineering, University of Technology, Dalian, China.

Her current research interests include signal processing in mmWave communications, MIMO communications, and multicasting systems.

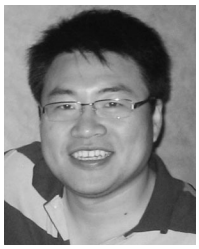

Ming Li (S'05–M'11–SM'17) received the M.S. and Ph.D. degrees in electrical engineering from the State University of New York at Buffalo (SUNY-Buffalo), Buffalo, NY, USA, in 2005 and 2010, respectively.

From January 2011 to August 2013, he was a Postdoctoral Research Associate with the Signals, Communications, and Networking Research Group, Department of Electrical Engineering, SUNY-Buffalo. From August 2013 to June 2014, he was with Qualcomm Technologies, Inc., as a Senior Engineer. Since June 2014, he has been with the School of Information and Communication Engineering, Dalian University of Technology, Dalian, China, where he is presently an Associate Professor. His current research interests include the general areas of communication theory and signal processing with applications to mmWave communications, secure wireless communications, cognitive radios and networks, data hiding, and steganography.

Qian Liu (S'09–M'14) received the B.S. and M.S. degrees from the Dalian University of Technology, Dalian, China, in 2006 and 2009, respectively, and the Ph.D. degree from the State University of New York at Buffalo (SUNY-Buffalo), Buffalo, NY, USA, in 2013.

From 2013 to 2015, she was a Postdoctoral Fellow with the Ubiquitous Multimedia Laboratory, SUNY-Buffalo. She received the Alexander von Humboldt Fellowship in 2015 and was a Postdoctoral Fellow at the Chair of Media Technology and the Chair of Communication Networks, Technical University of Munich, from 2016 to 2017. She is currently an Associate Professor with the School of Computer Science and Technology, Dalian University of Technology, Dalian, China. Her current research interests include multimedia transmission over MIMO systems, IEEE 802.11 wireless networks and LTE networks, device-to-device communication, energy-aware multimedia delivery, and the Tactile Internet. She received the Best Paper Runner-up Award at the 2012 IEEE International Conference on Multimedia and Expo and was in the finalist for the Best Student Paper Award at the 2011 IEEE International Symposium on Circuits and Systems.

A. Lee Swindlehurst (S'83–M'84–SM'89–F'04) received the B.S. and M.S. degrees in electrical engineering from Brigham Young University (BYU), Provo, UT, USA, in 1985 and 1986, respectively, and the Ph.D. degree in electrical engineering from Stanford University, Stanford, CA, USA, in 1991. From 1990 to 2007, he was with the Department of Electrical and Computer Engineering, BYU, where he was the Department Chair from 2003 to 2006. During 1996–1997, he held a joint appointment as a Visiting Scholar with Uppsala University and the Royal Institute of Technology, Sweden. From 2006 to 2007, he was on leave working as the Vice President of Research for ArrayComm LLC, San Jose, CA, USA. Since 2007, he has been a Professor with the Electrical Engineering and Computer Science Department, University of California Irvine, Irvine, CA, USA, where he was an Associate Dean for Research and Graduate Studies with the Samueli School of Engineering from 2013 to 2016. During 2014–2017, he was also a Hans Fischer Senior Fellow with the Institute for Advanced Studies, Technical University of Munich. His research interests include array signal processing for radar, wireless communications, and biomedical applications, and he has more than 300 publications in these areas. He was the inaugural Editor-in-Chief for the IEEE JOURNAL OF SELECTED TOPICS IN SIGNAL PROCESSING. He was a recipient of the 2000 IEEE W. R. G. Baker Prize Paper Award, the 2006 IEEE Communications Society Stephen O. Rice Prize in the Field of Communication Theory, the 2006 and 2010 IEEE Signal Processing Society's Best Paper Awards, and the 2017 IEEE Signal Processing Society Donald G. Fink Overview Paper Award.